TITLE A STUDY OF THE HIGH FREQUENCY STRUCTURE OF SPECTRAL LIGHT INTENSITY PRODUCED BY SPARK EXCITATION USING ELECTRON MULTIPLIER PHOTOTUBES

AUTHOR LYMAN WALTON ORR

UNIVERSITY OF MICHIGAN DATE 1949

DEGREE Ph.D. PUBLICATION NO. 1729

A STUDY OF THE HIGH FREQUENCY STRUCTURE OF SPECTRAL LIGHT INTENSITY PRODUCED BY SPARK EXCITATION USING ELECTRON MULTIPLIER PHOTOTUBES

Lyman W. Orr

A Dissertation Submitted in Partial Fulfillment
of the Requirements for the Degree of
Doctor of Philosophy in the
University of Michigan
1949

Committee in Charge:
Professor L. N. Holland, Chairman
Professor S. S. Attwood
Professor R. V. Churchill
Professor W. G. Dow
Professor R. A. Wolfe

ACKNOWLEDGEMENT

The author wishes to express his gratitude to Professor R. A. Wolfe for his encouragement and valuable advice, to Dr. J. H. Enns for his helpful discussions, and to Professor L. N. Holland for his advice and assistance in the early part of the work.

The work herein described has been conducted under the sponsorship of the Bethlehem Steel Company, Bethlehem, Pennsylvania.

TABLE OF CONTENTS

TABLE OF CONTENTS (continued)

LIST OF ILLUSTRATIONS

I. THE PROBLEM

In the field of quantitative spectrographic analysis considerable accuracy has been achieved. Efforts to improve this accuracy to its ultimate limit are continually being sought. There are two general lines of research to be followed in improving the accuracy, (a) by refining the intensity measurements on the spectral lines, and (b) by improving the reproducibility of the excitation used to generate the spectral energies to be measured.

In industrial control analysis, fairly good accuracy is obtained in many cases using the photographic technique, and more recently, using direct reading devices[1,2,3,4]. To illustrate the methods employed, suppose it is desired to obtain the percent concentration of an element X in a sample containing a control element A. In metal samples the matrix element of the sample is usually chosen as the element A. Two suitable spectral lines are chosen having intensities I_x and I_a which are due to the presence of elements X and A. If the concentration of the element A is substantially constant, the intensity ratio $I_x : I_a$ will be in direct proportion to the concentration of the element X. The proportionality constant will depend upon the lines chosen, and may be found by the use of standard samples of known chemical composition.

In the photographic method, the spectrum is exposed to a suitable photographic emulsion for a period of t seconds. The emulsion is processed and the densities D_x and D_a of the lines are read on a microdensitometer. From these readings the intensity ratio $I_x : I_a$ may be calculated.

In the direct reading method, the spectral lines to be measured are allowed to fall upon the cathodes of two electron multiplier phototubes for a suitable period of t seconds. The photocurrents J_x and J_a are compared by means of an electronic circuit which produces a dial reading varying with the intensity ratio $I_x : I_a$. This dial may be directly calibrated in percent X.

In 1942, Vincent and Sawyer[5] showed that in the analysis of chromium in steel, deviations in the analytical results were attributable largely to variations in the excitation conditions when the source constants were fixed. Thus a point has been reached where further improvements in the precision of intensity measurements of the lines result in only minor improvements in overall accuracy. The most profitable course therefore appears to be in the improvement of reproducibility in exciting the spectral energies.

For quantitative analysis of metals, the sample is usually a pair of cylindrical pins 3/16 to ¼ inch in

diameter. These are ground at the tips to a standard shape, and placed in clamps to form a gap. A spark current is passed through this gap which evaporates metal from the tips and excites the resulting vapor. The light energy is analyzed by means of a spectrograph. In cases where the concentration of the element to be determined is very small, arc excitation is used. But in general, spark excitation gives more uniform sampling of the pins, and better accuracy in the analysis. Arc currents used are of the order of 3 to 12 peak amperes, while spark currents used are from 100 to 1000 peak amperes. The duration of current flow per spark is relatively short, ranging from 10 to 100 microseconds.

Changes in the standard deviation of quantitative results with changing source conditions may be studied by the photographic method. The method is tedious, for many months of work are required to obtain adequate data for such calculations. Although valuable information is obtained about the optimum source conditions for industrial control analysis, the method gives little information about the basic causes of the variations. The problem is further complicated by the fact that different optimum conditions are found for different alloys, and frequently for different elements in the same alloy. To find the causes of these discrepancies, one must obtain more

knowledge of the mechanism involved in excitation. The present work is therefore devoted to the study of intensity variation of certain spectral lines during the short interval of spark current flow, and its relation to this current. It is hoped that this will lead to a better understanding of the mechanism involved.

II. APPARATUS

A. GENERAL REQUIREMENTS

1. Cathode ray equipment for simultaneous recording of the light intensity variations and spark current of a single spark or series of sparks.

2. A suitable pickup to convert the light pulses into electrical impulses which is sensitive in the ultraviolet and has adequate frequency response to detect the variations sought.

3. A suitable wide band amplifier of sufficient gain to produce deflection voltages from these electrical impulses.

4. A driven sweep synchronized with the beginning of the spark, and a gating arrangement, so that any particular spark in the cycle may be preselected and displayed either once only for photographic recording, or repeated at a 60 cycle rate for visual study.

5. The apparatus must not be affected adversely by the strong radiofrequency electromagnetic field present near the spark source.

B. DESCRIPTION OF APPARATUS

1. A general layout of the apparatus is shown in Fig 1. A current pickup R is inserted in the spark

Fig 1.

GENERAL LAYOUT OF APPARATUS

R is a high wattage non inductive resistor used as a current pickup.

P is the Phototube Unit serving as the light pickup.

C1 and C2 are coaxial cables each terminated by an appropriate terminating resistance R_t.

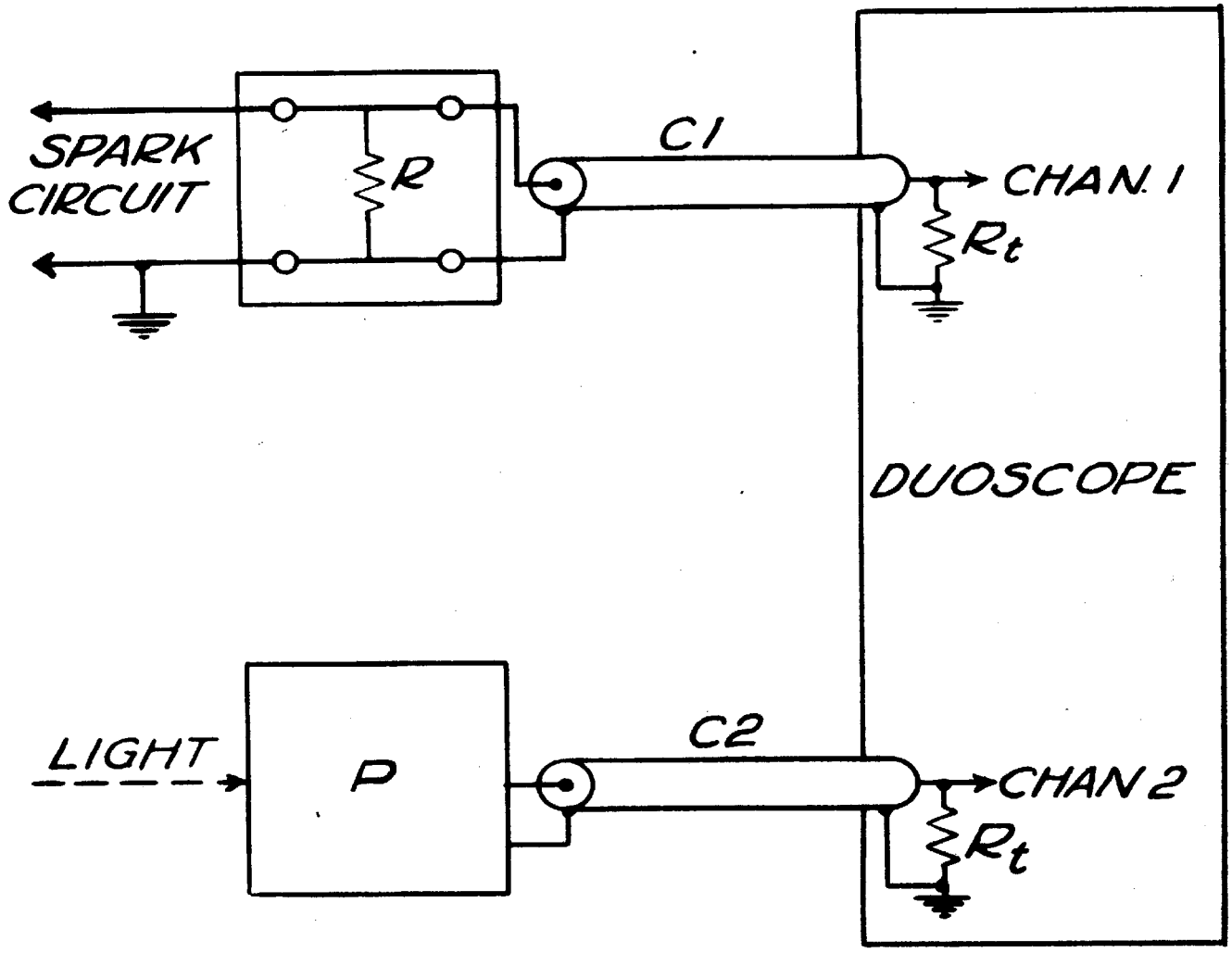
SPARK
CIRCUIT
R
C1
CHAN. 1
R_t
DUOSCOPE
LIGHT
P
C2
CHAN 2
R_t

circuit close to the sample gap. Its potential terminals are connected to one channel of the Duoscope by a properly terminated coaxial cable C1. The phototube unit P, located on the spectrograph, is similarly connected to the other channel of the Duoscope. Each terminating resistance R_t was adjusted to within 2% of the characteristic impedance of the coaxial cable as quoted by the manufacturer. Distortion of signals due to standing waves or reflections in the cables was thereby avoided.

2. Current Pickup. A non inductive resistor capable of carrying the high peak spark current and of dissipating the heat was required. Since RMS spark currents of 10 amperes were commonly used, a dissipation of 100 watts is required for a one ohm resistor.

To give a true representation of current, the device must have an inductive reactance which is small compared to its resistance at the highest frecuency employed. In general, spark current frequencies are not in excess of one megacycle per second, and at this frequency an inductance of 10^{-8} henries would present an impedance of $j2\pi \times 10^{-2}$ ohms. For a one ohm resistor this was considered small enough so that errors due to inductive effects could be ignored.

Several of these resistors were constructed having resistances from 1.0 ohm to 0.1 ohm. The method of

construction is shown in Fig 2. The resistance element R is a length of *Copel Ribbon ¼ inch wide and .005 inch in thickness. It has a resistance of .185 ohms per foot, and a negligible percent increase in resistance between 68° F and 900° F according to the manufacturer[6]. The ribbon is folded back and forth over a span of about two inches, and the folds interleaved with sheets of mica M, approximately .001 inch in thickness. The whole is then firmly clamped between two heavy brass plates BB, which serve as the terminals and provide the necessary heat radiating area. The clamping provides good thermal contact between the resistance element and the terminal plates. Separate current and potential terminals are provided.

It is to be noted that the magnetic flux around any section of the resistance element is confined to a cross-section area of about .002 square inches, while the length of the flux path is more than ½ inch. This feature gives the extremely low inductance required. The inductance of the one ohm resistor was measured at several frequencies from 25 to 75 megacycles on a high frequency Q meter by the substitution method. The average inductance thus found was 1.1×10^{-8} henries.

*Copel: an alloy of 55% Cu and 45% Ni.

Fig 2.

CONSTRUCTION OF NON INDUCTIVE RESISTOR

R Resistance element, Copel ribbon

M Mica sheets

BB Brass plates

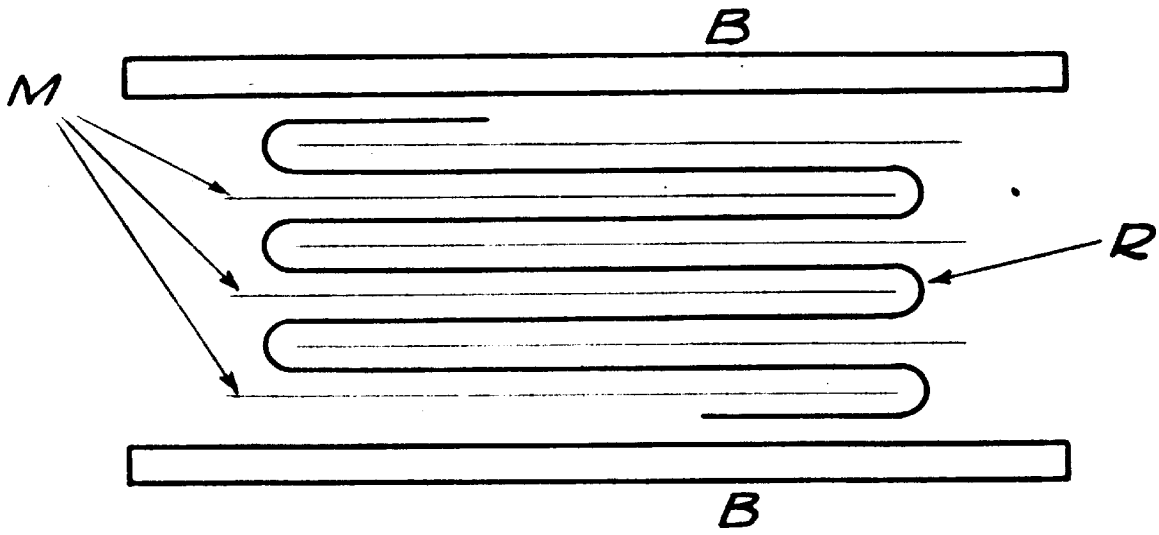
B
M
R
B

3. Phototube Unit. The Type 1P28 electron multiplier phototube was housed in a light-tight brass housing together with an attenuator, band-limiting switch and cathode follower. Light from the Bausch and Lomb quartz spectrograph was admitted through a slit located in the focal plane of the instrument. The effective slit width was about 100 microns. An adjustable, front-surface-aluminized mirror was used to direct the light passing through the slit to the most sensitive portion of the phototube cathode surface. Horizontal motion of the slit and housing was obtained by means of a lead screw and micrometer head.

The electrical circuit of the unit is shown in Fig 3. The 1600 ohm anode load of the phototube is tapped to provide attenuation in factors of 2. The output of the attenuator switch S2 is fed to the grid of a 6J4 cathode follower which makes an appropriate impedance transformation to feed the coaxial cable. The cathode load consists of the cable and its terminating resistance R_t. The band limiting switch S1 inserts various condensers in parallel with the phototube load resistor to provide bandwidths of 0.1, 0.3, 1, 3 and 10 megacycles. Condenser values were chosen to produce 70% response at these frequencies. No condenser is required for the 10 megacycle position of S1 since the bandwidth is here limited by the tube and circuit capacities which are in parallel with the anode load.

Fig 3

CIRCUIT OF PHOTOTUBE UNIT

Resistor values are given in ohms unless marked K for thousands or M for megohms. Resistor ratings are ½ watt unless otherwise specified.

Condenser values are in microfarads unless marked PF for picofarads = micromicrofarads. Polarity marks indicate electrolytic condensers.

Filament and plate current for the 6J4 cathode follower, and phototube voltage are supplied through a shielded cable.

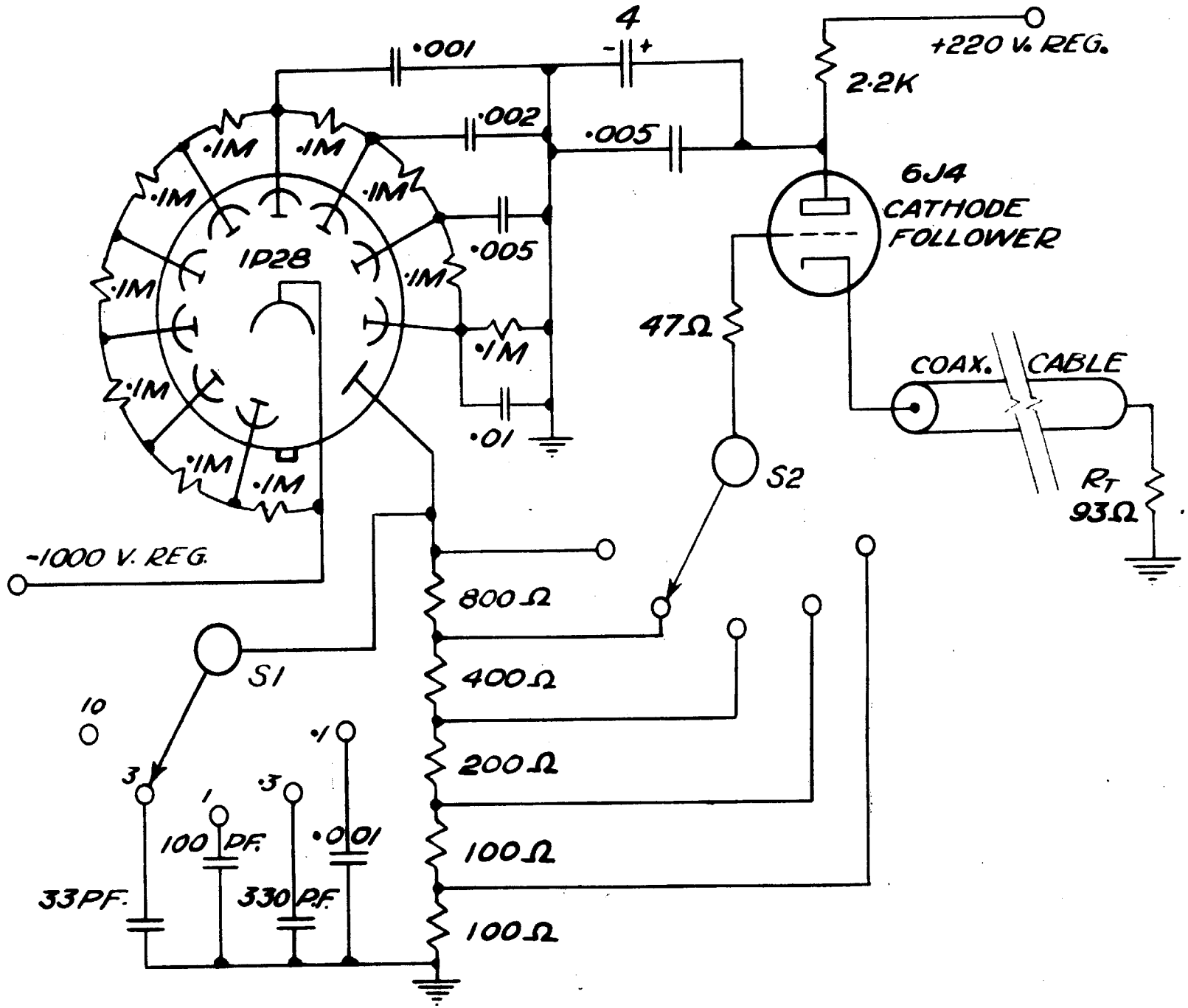
4
.001
.002
.005
.005
.01
.1M
.1M
.1M
.1M
.1M
.1M
.1M
.1M
1P28
+220 V. REG.
2.2K
6J4
CATHODE
FOLLOWER
47Ω
COAX. CABLE
RT
93Ω
S2
-1000 V. REG.
800Ω
400Ω
200Ω
100Ω
100Ω
S1
10
3
1
.3
.1
100 PF.
.001
33PF.
330 PF.

The cathode follower is supplied with a regulated voltage of 220 volts. This is dropped to 190 volts at the plate by the decoupling filter consisting of the 2.2 K resistor and 4 uf electrolytic condenser. The .005 uf mica condenser is connected directly at the plate pin of the socket, providing a good RF ground at this point. Decoupling is required to prevent the introduction of spurious signals picked up by the power cable. The gain of the cathode follower is approximately 0.5. A phototube anode current pulse of one milliampere produces a voltage pulse of 0.8 volts across R_t with S2 set for no attenuation.

The phototube dynode potentials are provided by a regulated voltage of -1,000 volts and a bleeder consisting of ten .1 megohm resistors. Since the photocurrent pulses are rather large compared to the average current, filter condensers are provided for the last four dynodes. This assures that dynode voltages will not change appreciably during the pulse of photocurrent. Assuming a stage gain of 3, and an anode current pulse of one milliampere lasting 50 microseconds, one may calculate the change in voltage on dynode 9 as follows. The current in this dynode will be the anode current minus the current contributed by dynode 8. Since the stage gain is 3, the net current in

dynode 9 will be 2/3 of the anode current or 0.67 ma.

The change in voltage at dynode 9 will be given by

$$\Delta E = \frac{1}{C} \int_0^t i\,dt = \frac{it}{C}$$

and on inserting the values C = .01 uf., i = .67 ma., and t = 50 usec., one obtains ΔE = 3.3 volts. Similar calculations for the other dynodes to which condensers are connected give the following values of ΔE for the assumed conditions.

Dynode No	C	ΔE
8	.005 uf	2.2 volts
7	.002	1.85
6	.001	1.25

Condensers are not required by the other dynodes since the currents are much smaller here. For instance the current in dynode 5 is 9 microamperes for the assumed conditions, and the change in voltage here due to changes in the IR drops in the bleeder resistors is less than one volt. No appreciable error will be introduced in intensity patterns by voltage changes of the magnitudes mentioned.

4. Duoscope. The Duoscope is a two channel synchroscope with coupled horizontal sweeps. A block diagram of the Duoscope Equipment is shown in Fig 4. The light lines and arrows on the diagram indicate the flow of DC power and heater current to the various units. The heavy lines and

Fig 4

BLOCK DIAGRAM OF DUOSCOPE APPARATUS

Units in the first three columns at the left comprise the indicator chassis or Duoscope proper.

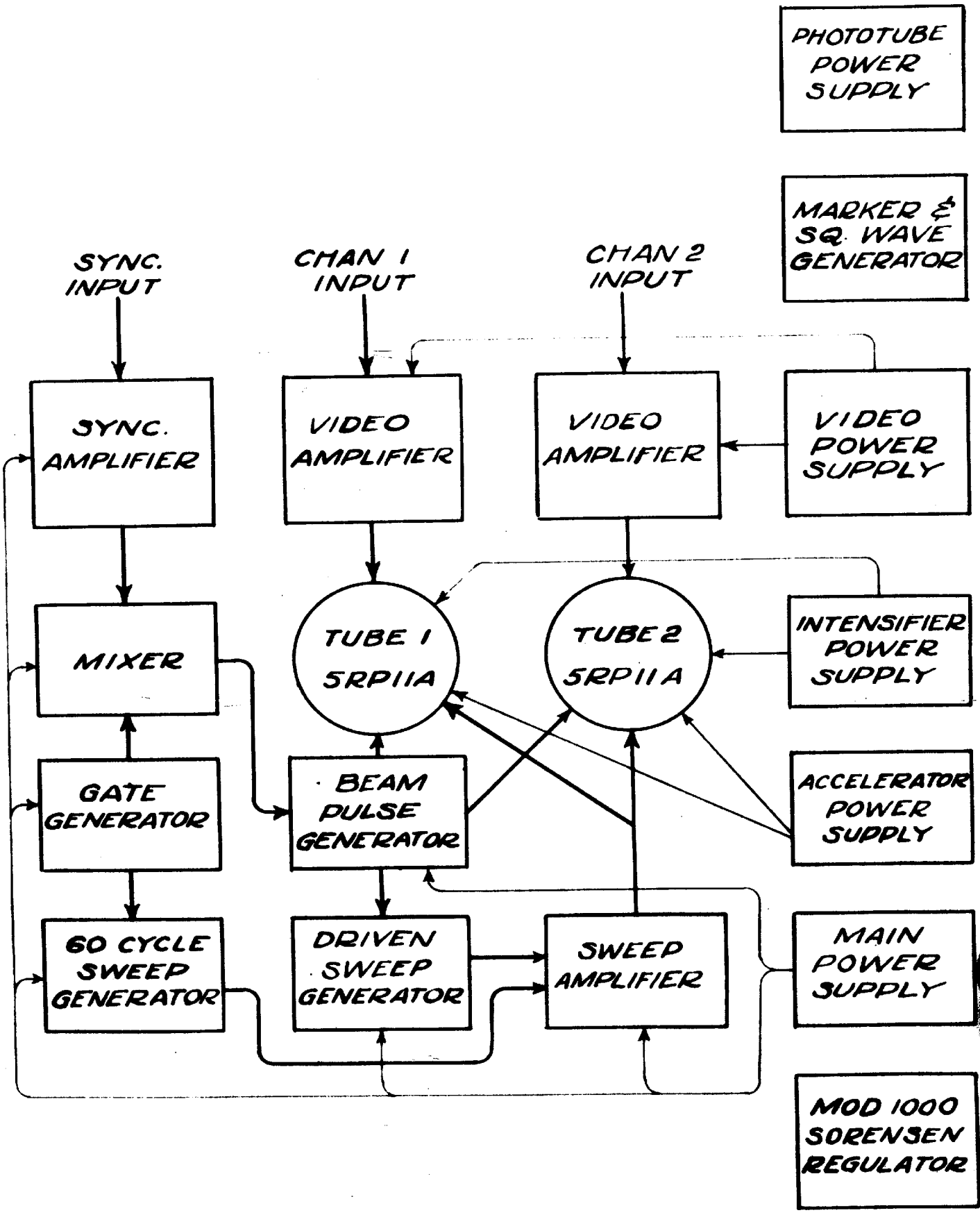
PHOTOTUBE POWER SUPPLY
MARKER & SQ. WAVE GENERATOR
SYNC. INPUT
CHAN 1 INPUT
CHAN 2 INPUT
SYNC. AMPLIFIER
VIDEO AMPLIFIER
VIDEO AMPLIFIER
VIDEO POWER SUPPLY
MIXER
TUBE 1 5RP11A
TUBE 2 5RP11A
INTENSIFIER POWER SUPPLY
GATE GENERATOR
BEAM PULSE GENERATOR
ACCELERATOR POWER SUPPLY
60 CYCLE SWEEP GENERATOR
DRIVEN SWEEP GENERATOR
SWEEP AMPLIFIER
MAIN POWER SUPPLY
MOD 1000 SORENSEN REGULATOR

Fig 5.

PHOTO OF DUOSCOPE EQUIPMENT

Units are mounted on a standard five foot transmitter rack.

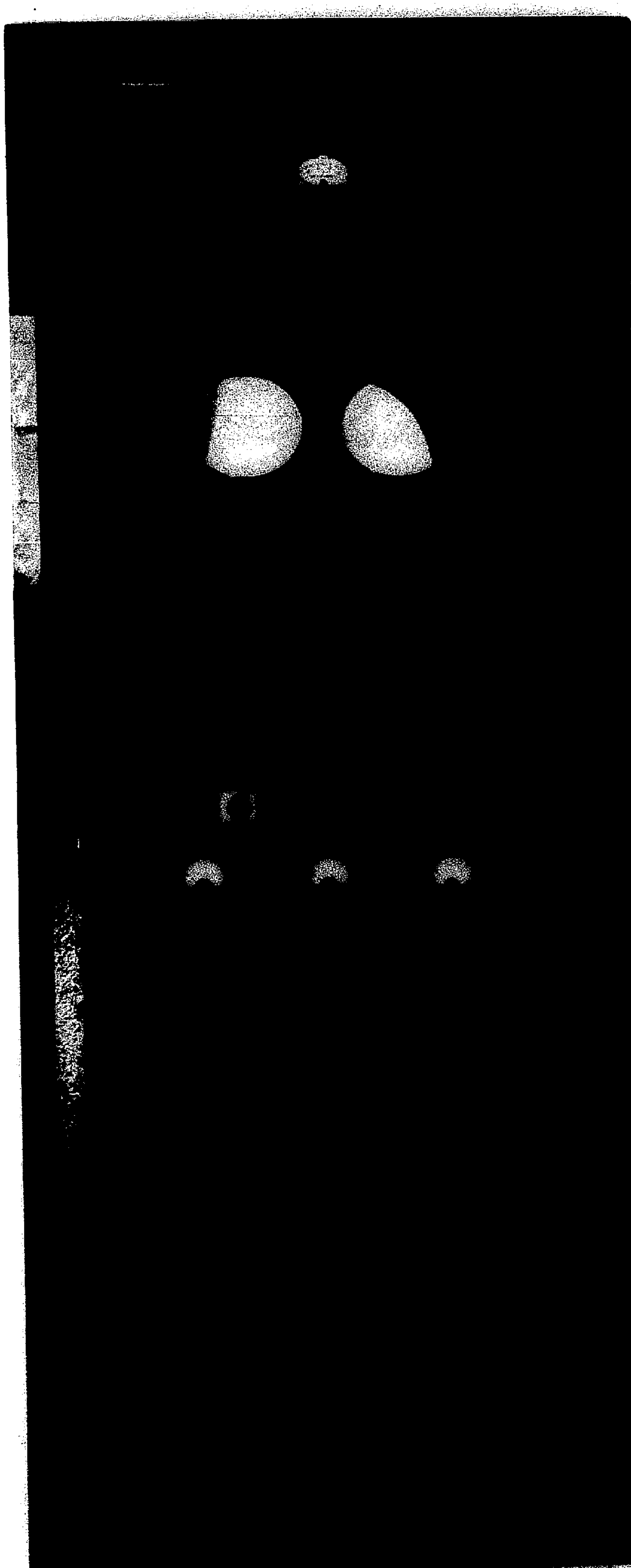

arrows indicate the paths taken by the signals and pulses.

With the exception of the Video Power Supply, the units in the right hand column are powered from the Model 1000 Sorensen Regulator at the bottom. This provides power at a steady voltage of 115 volts regardless of line voltage fluctuations. The units in the first three columns at the left, including the two Dumont 5RP11A cathode ray tubes, comprise the indicator chassis or Duoscope proper. The units are mounted on a standard five foot transmitter rack as illustrated in Fig 5.

Each of the units will now be considered in detail, and the operation of the whole will be summarized in Section C.

5. Cathode Ray Tubes. Since it was desired to display two traces simultaneously, a double gun cathode ray tube such as the 5SP was considered. However a relatively high beam intensity was required for photographic recording of single events at the high writing speeds involved, and for this an intensifier voltage of about ten kilovolts was required. Since the 5SP is not designed for this high a voltage, it had to be abandoned.

In most cathode ray tubes of the post deflection intensifier type such as the 5CP, the ratio $R = E_3/E_2$ may not exceed about 2.3 without producing an objectionable deflection distortion[7]. Here E_3 represents the voltage of

the final anode, and E_2 that of the second anode, both measured from the cathode. However by using a special arrangement of the intensifier anodes and a different construction[7], the 5RP11A tube permits satisfactory operation at R = 10 and values of E_3 up to 25 kilovolts.

At the time of constructing the apparatus, the 5RP types were not available in double gun models, and therefore it was necessary to use two separate 5RP11A tubes. These were operated at E_2 = 1.5 kilovolts, and E_3 = 10 kilovolts giving R = 6.7. With these operating conditions a deflection factor of about 90 DC volts per inch was obtained with no noticeable deflection distortion. Separate focus and intensity controls were provided for each tube.

6. Video Amplifiers. Two video amplifiers are provided, one for each channel of the instrument. The circuit diagram is shown in Fig 6, and is the same for both amplifiers. Their frequency response is flat within 2 decibels between 10 cycles and 6 megacycles as indicated by the curve in Fig 7.

In Fig 6, Switch S1 at the input terminals provides a 93 ohm input resistance for correct termination of the coaxial cable. With S1 open, the effective input impedance is approximately one megohm in parallel with 26 uuf. The three position switch S2 provides attenuation ratios of

Fig 6.

VIDEO AMPLIFIER CIRCUIT

Resistor values are given in ohms unless marked K for thousands or M for megohms. Resistor ratings are ½ watt unless otherwise specified.

Condenser values are in microfarads unless marked PF for picofarads = micromicrofarads. Polarity marks indicate electrolytic condensers.

Inductances are given in microhenries and are slug tuned. They have a rating of 100 milliamperes.

CRT represents the Cathode Ray Tube.

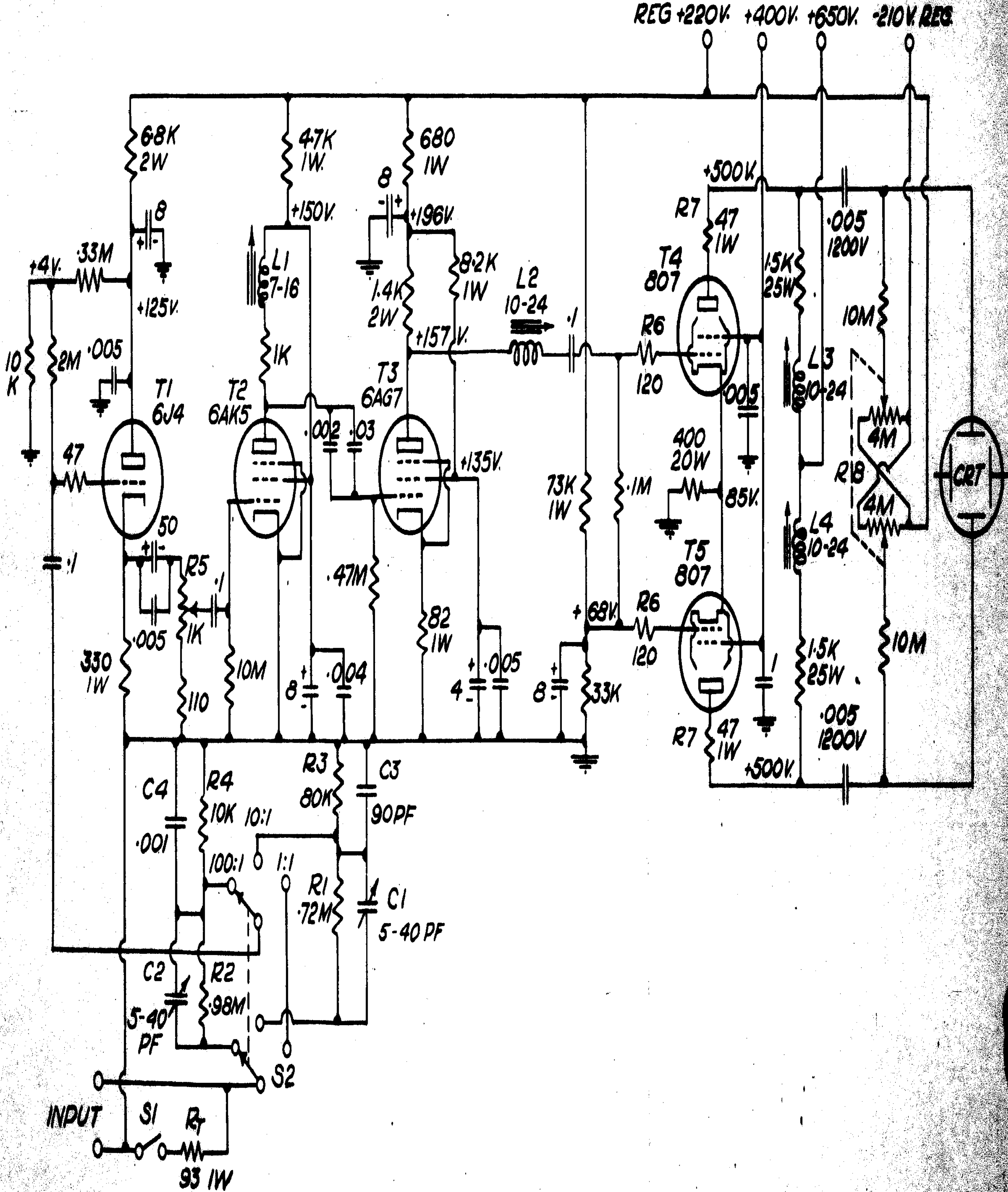

REG +220V.
+400V.
+650V.
-210V. REG.
6.8K
2W
47K
1W.
680
1W
8
+4V.
.33M
+125V.
+150V.
+196V.
L1
7-16
1.4K
2W
8.2K
1W
L2
10-24
.1
+500V.
R7
47
1W
T4
807
1.5K
25W
.005
1200V
10M
10
K
2M
.005
T1
6J4
1K
T2
6AK5
+157V.
T3
6AG7
R6
120
L3
10-24
.005
.002
.03
+135V.
73K
1W
.1M
400
20W
85V.
R8
4M
4M
CRT
47
50
L4
10-24
.1
R5
1K
.1
.47M
T5
807
.005
330
1W
10M
82
1W
+
68V.
R6
120
1.5K
25W
110
8
.004
4
.005
8
33K
1
.005
1200V
R7
47
1W
+500V.
C4
.001
R4
10K
R3
80K
C3
90PF
10:1
100:1
1:1
R1
.72M
C1
5-40 PF
C2
5-40
PF
R2
.98M
S2
INPUT
S1
RT
93 1W

Fig 7.

FREQUENCY RESPONSE OF VIDEO AMPLIFIERS

The zero decibel level in the diagram corresponds to a mid-frequency voltage gain of approximately 250.

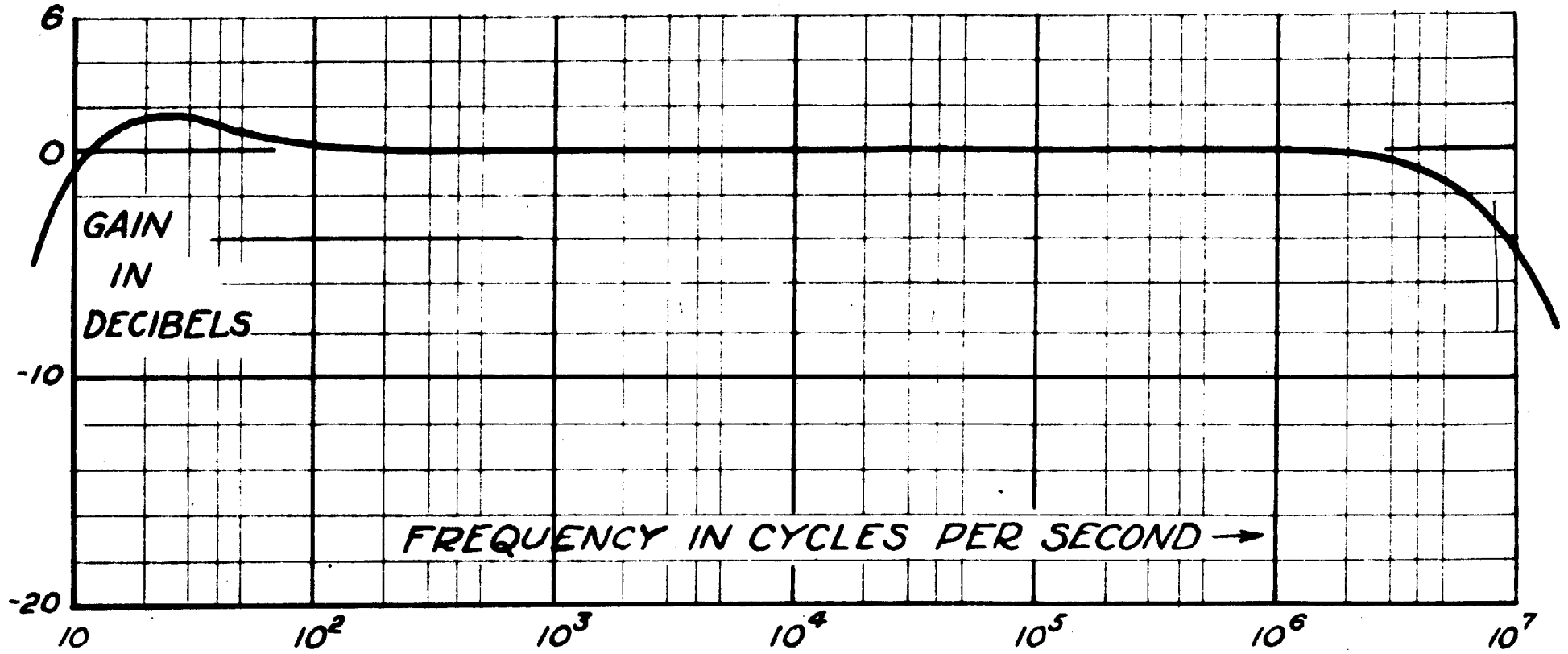
6
0
-10
-20
GAIN
IN
DECIBELS
FREQUENCY IN CYCLES PER SECOND →
10
10²
10³
10⁴
10⁵
10⁶
10⁷

100:1, 10:1, and 1:1. The condenser and resistor values are chosen to satisfy the relations

$$\frac{R1}{R3} = \frac{C + C3}{C1} = 10 \qquad (1)$$

$$\frac{R2}{R4} = \frac{C + C4}{C2} = 100 \qquad (2)$$

which are necessary for equal attenuation of high and low frequencies. C represents the capacity of the attenuator output circuit. The method of adjusting the trimming condensers C1 and C2 is described in the next section.

The output of the attenuator is coupled to the grid of cathode follower T1. The cathode is coupled to R5 which serves as the gain control. The moving contact of R5 is coupled to the grid of the first amplifier tube T2. The type 6AK5 tube used here has a gold plated grid, and is therefore subject to considerably less electron emission from the grid than conventional grids placed in such close proximity to the hot cathode. A large grid circuit impedance is therefore permissible. With a 10 megohm grid leak, the tube develops between 0.5 and 0.8 volt negative bias due to Edison effect, and obviates the need for other biasing arrangements.

The remainder of the amplifier was designed in accordance with conventional video design methods described by

Terman[8]. A top frequency of 8 megacycles was chosen as a design figure. A two terminal coupling network was used between T2 and T3 while a four terminal network was used between T3 and T4. The centre values of the slug tuned peaking coils L1, L2, L3 and L4 were calculated to give circuit Q's of approximately 0.7. Commercially available slug tuned HF oscillator coils were rewound to give the proper values. The adjustment of the peaking coils is described in the next section.

The final amplifier stage is a push-pull pair of 807 tubes, T4 and T5. The grid of T5 is held at a steady DC potential of 68 volts. The grid of T4 is driven by the output of T3, and cathode coupling of T4 and T5 is used to provide the required inversion for push-pull operation. The 807 tube is rated by the manufacturer at 30 watts maximum plate dissipation, but overrating tests showed that satisfactory tube life for intermittent operation was obtained even at 50 watts. The amplifier was designed so that the plates of the 807's would dissipate 40 watts each. Parasitic suppressing resistors R6 and R7 were used in series with the grid and plate of each 807.

The double 4 megohm potentiometer R8 serves as the vertical position control, and a switch (not shown) disconnects the amplifier and provides direct connection to the deflection plates through a separate input terminal when desired.

7. Adjustment of Peaking Coils and Attenuator Trimming Condensers

The peaking coils L1 to L4 of the video amplifiers were adjusted with the aid of a 100 kilocycle square wave generator having low output impedance. The adjustment in each case was made to produce the fastest rise in the leading edge of the square wave without overshoot as viewed on the screen of the cathode ray tube. The square wave was first applied to the grid of T4 with T3 removed from its socket. L3 was adjusted with the lower deflection plate (in Fig 5) grounded. Then L4 was adjusted with the upper deflection plate grounded. Settings were then checked with the ground removed. T3 was replaced in its socket and T2 removed. The square wave was applied to the plate pin socket of T2 and L2 adjusted. T2 was replaced and S2 set in the 1:1 position. The square wave was then applied to the input and L1 adjusted.

The adjustment of the trimming condensers C1 and C2 was then made. This was done in a similar manner except that a 10 kilocycle square wave was used. This wave was applied to the input terminals with S1 open. With S2 in the 100:1 position, C2 was adjusted for the most faithful reproduction of the square wave. With S2 in the 10:1 position, C1 was similarly adjusted. The appearance of attenuator response to the 10 kc square wave for different condenser settings is shown in Fig 8.

Fig 8.

ATTENUATOR RESPONSE TO 10 KILOCYCLE SQUARE WAVE AT DIFFERENT SETTINGS OF TRIMMING CONDENSER

A. Trimming condenser set high

B. Trimming condenser set low

C. Proper adjustment

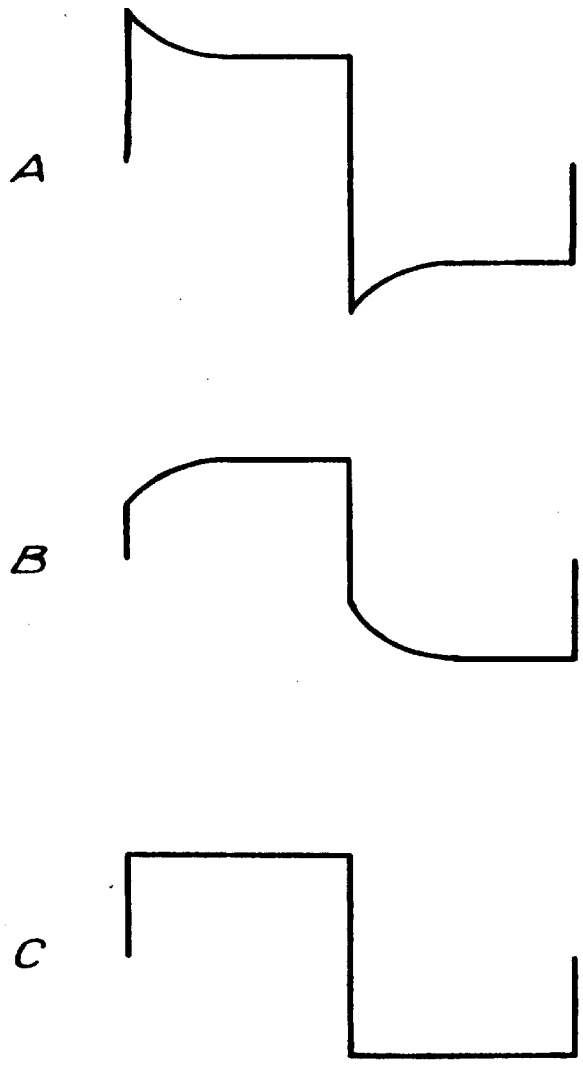
A
B
C

8. Gate Generator. This circuit provides a means of selecting a portion of the cycle for study at the exclusion of other portions. A phase shift control permits the selected portion to be shifted manually to any phase position in the cycle. The method employed is to generate a gate pulse which is fed to one channel of a coincidence circuit or mixer tube, while the synchronizing signal is applied to the other channel. The operation of the mixer is discussed in part 10 of this section.

The circuit of the Gate Generator is shown in Fig 9. Tubes T1 and T2 are overdriven amplifiers which produce at the right hand plate of T2 a 60 cycle square wave which is in phase or 180° out of phase with the line frequency depending upon the position of switch S1. This square wave is differentiated by an RC circuit so that a peaky wave results. The peaky wave is composed of a positive and a negative "pip" of voltage. The crystal diode X_1 offers a low shunting resistance to ground for the positive pip, but a rather high resistance to the negative pip. The resulting wave at the anode of X_1 is a very small positive pip followed a half cycle later by a rather large negative pip. This RCX circuit which converts square waves into negative pips is used several times in the Gate Generator. The negative pip coincides in time with the negative going portion of the applied square wave. The very small positive

Fig 9.

GATE GENERATOR CIRCUIT

Resistors are given in ohms unless marked K for thousands or M for megohms. Resistor ratings are ½ watt unless otherwise specified.

Condenser values are in microfarads unless marked PF for picofarads = micromicrofarads. Polarity marks indicate electrolytic condensers.

X_1 and X_2 are Type 1N34 Germanium Crystal Diodes.

B is the control button for Manual Gate.

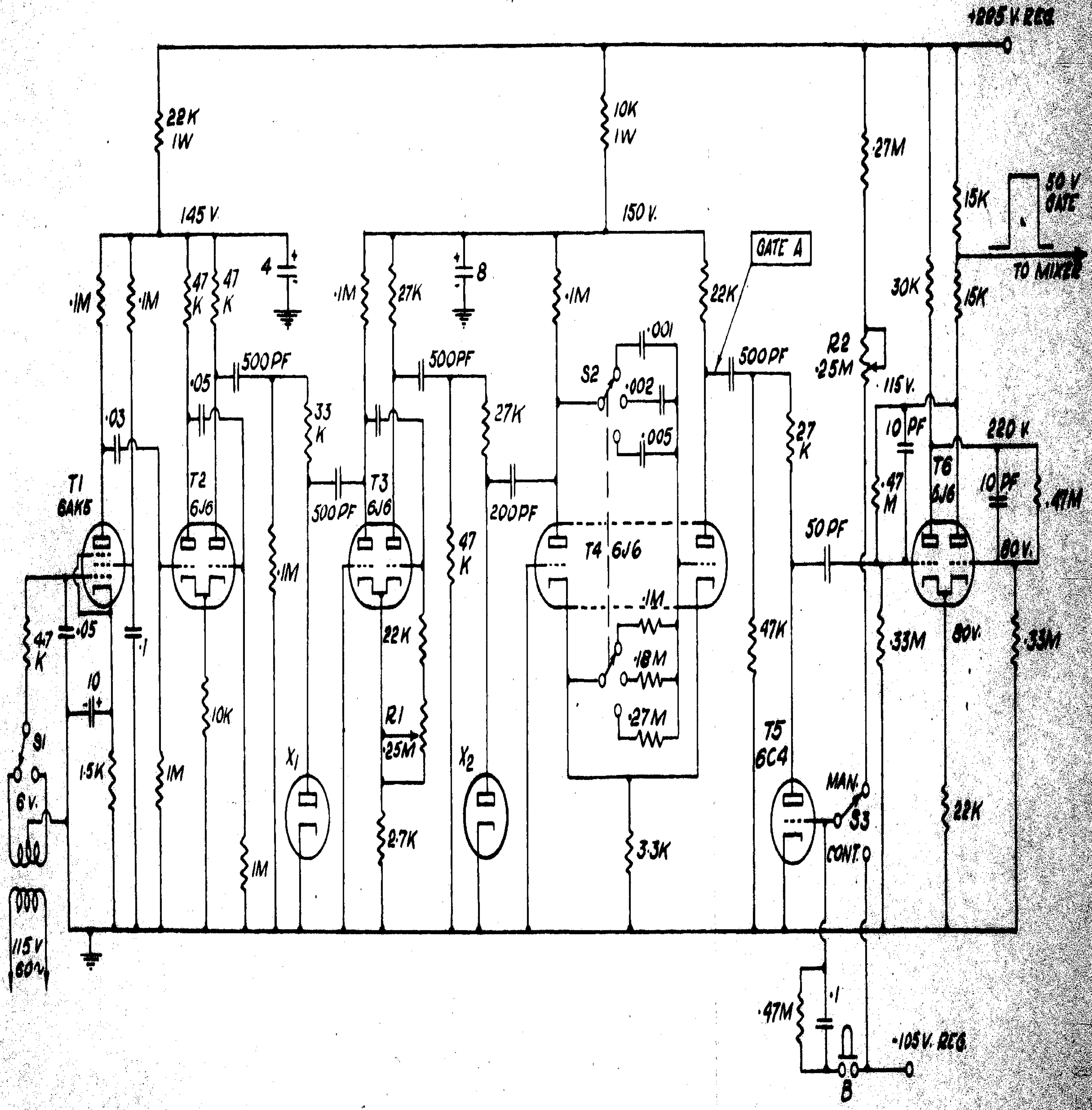
+225 V. REG.
22K 1W
10K 1W
145 V
150 V.
.27M
15K
50 V GATE
TO MIXER
GATE A
4
8
.1M
.1M
47 K
47 K
.1M
27K
.1M
22K
30K
15K
500 PF
500 PF
500 PF
.001
S2
.002
.005
R2 .25M
115 V.
10 PF
220 V.
.05
.03
33 K
27K
27 K
.47 M
T6 6J6
10 PF
.47M
T1 6AK5
T2 6J6
T3 6J6
500 PF
200 PF
47 K
T4 6J6
50 PF
80 V.
.1M
.1M
.05
.1
47 K
22 K
.18M
47K
.33M
80V.
.33M
10
S1
R1 .25M
.27M
10K
1.5K
1M
X1
X2
T5 6C4
MAN.
S3
22K
6 V.
1M
2.7K
3.3K
CONT.
115 V 60~
.47M
.1
-105 V. REG.
B

pip is of no consequence.

The negative pip at X_1 is used to trip a single-shot delay multivibrator T3. The control resistance R1 provides manual adjustment of the period of conduction of the left hand unit of T3. At the conclusion of this period, the right hand unit resumes conduction and its plate voltage drops suddenly. A second RCX circuit connected to this plate produces a negative pip at the anode of X_2 which may be shifted in phase through 220 electrical degrees by the control R1. Since a phase shift of 180° is available at S1, it is clear that one may adjust this pip to any desired phase position in the cycle.

The gate multivibrator T4 is tripped by this negative pip which is applied to the left hand plate. Since the right hand unit of T4 is normally conducting, a positive rectangular gate pulse (GATE A) is formed here when tripping occurs. S2 provides three different RC values in the grid decay circuit resulting in gate lengths of 0.3, 1.0 and 3.0 milliseconds.

If continuously gated operation were sufficient, GATE A could be used directly. However it is desired on occasion to record a single event in a series of events. In such a case the camera shutter would have to be carefully synchronized in order to be sure of obtaining only one event in the series. A more facile method is to prevent the gate

from acting in its normal way, and provide a manual control permitting a single gate to be passed in the proper phase to the mixer tube.

This feature is provided by tubes T5 and T6 and their associated circuits. When switch S3 is in the MAN (manual) position, T5 is at zero bias, and the circuit behaves like the RCX Circuits previously described, only negative pips being permitted to pass. When button B is pressed, the T5 grid voltage drops at once to -105 volts, and begins to decay back to zero. The RC network connected to the grid of T5 is adjusted by varying R2 so that the grid voltage decays back to zero in exactly 1/60 second. During this period of negative bias, there will be one positive pip of normal size permitted to form at the T5 plate. All successive positive pips will be spoiled by the low plate resistance of T5 since its grid has returned to a zero bias condition. T5 is called the Spoiler Tube for this reason.

When switch S3 is in CONT (continuous) position, the T5 grid is biased at a steady -105 volts, and both positive and negative pulses are now always unspoiled.

T6 is in a modified Eccles-Jordan or flip-flop circuit, which differs from the multivibrators in that stable conditions may exist when either unit of the tube is conducting. Let us suppose the left hand unit to be conducting and a

series of negative pips then be applied to the left grid. The first negative pip would transfer conduction to the right hand unit, and all subsequent negative pips would have no effect. However if one positive pip be introduced in this series, of sufficient size to initiate current in the left hand plate, conduction would be tripped to the left side. The next negative pip arriving at the left grid would again trip conduction to the right hand unit. The right hand plate will thus execute a positive gate pulse which begins with the arrival of a positive pip and ends with the arrival of the next negative pip.

It is now clear that in manual operation, no change in the output of T6 occurs until button B is pushed. However the first <u>complete</u> GATE A to occur subsequent to the pressing of button B is regenerated by T6; the method prevents <u>only a part</u> of GATE A being obtained. On continuous operation, every GATE A is regenerated by T6, for now <u>all</u> the positive pips are unspoiled by T5. The output gate pulse is taken from a tap in the plate load resistor of the right hand unit of T6. This pulse will hereafter be referred to merely as the Gate.

<u>9. Synchronizing Pulse Amplifier.</u> The input triode T1 of this circuit which is shown in Fig 10 acts as a cathode follower having gain control R1 as its cathode load. The output of the gain control is amplified by T2, inverted

Fig 10

SYNCHRONIZING PULSE AMPLIFIER CIRCUIT

Resistors are given in ohms unless marked K for thousands or M for megohms. Resistor ratings are ½ watt unless otherwise specified.

Condenser values are in microfarads unless marked PF for picofarads = micromicrofarads. Polarity marks indicate electrolytic condensers.

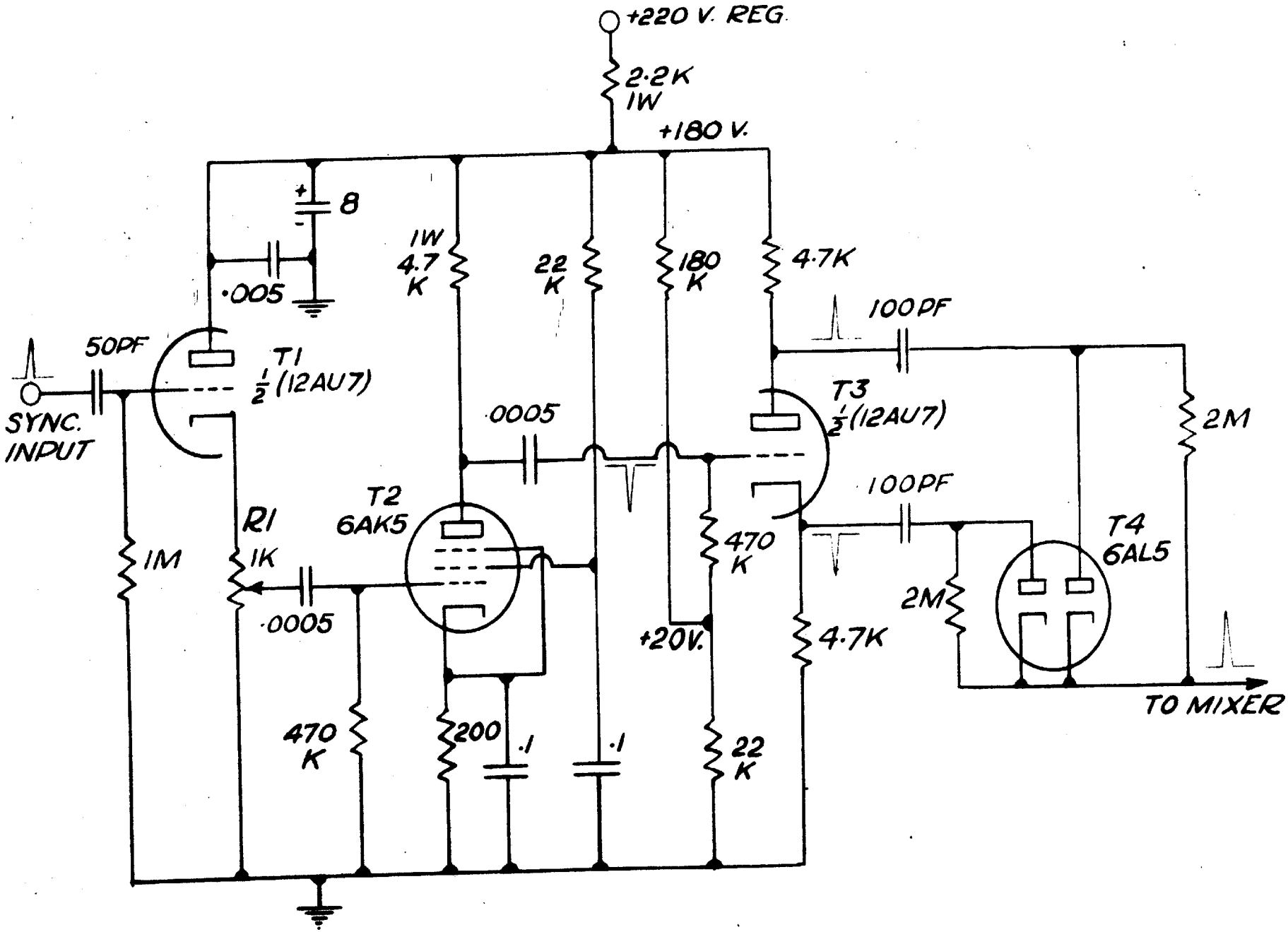
+220 V. REG.
2.2K
1W
+180 V.
8
.005
1W
4.7
K
22
K
180
K
4.7K
100PF
50PF
T1
½ (12AU7)
SYNC.
INPUT
.0005
T3
½ (12AU7)
2M
T2
6AK5
R1
1K
1M
100PF
470
K
T4
6AL5
2M
.0005
+20V.
4.7K
470
K
200
.1
.1
22
K
TO MIXER

by the cathodyne tube T3, and rectified by the full wave rectifier T4. The object is to produce a positive output pulse for an input pulse of either sign. The size of the output pulse may be controlled by adjusting R1.

10. Mixer or Coincidence Circuit. Fig 11 shows the mixer circuit consisting of a 6BE6 pentagrid tube. This tube is so constructed that a virtual cathode is formed in the region of grid 3. If grid 3 is about 40 volts negative with respect to the cathode, all electrons approaching from the cathode are repelled and collected by the positive grid 2. If grid 3 is at cathode potential, the bulk of electrons approaching it are passed on to the plate.

The two inputs to this circuit are (1) the positive pulse from the Synchronizing Pulse Amplifier, and (2) the Gate. These inputs are applied to grids 1 and 3 respectively of the 6BE6. The bias voltages are so adjusted that virtually no plate current will flow unless there is coincidence between the synchronizing pulse and the Gate. When this occurs, a negative Tripping Pulse is formed at the plate. This is used to trip the Beam Brightening and Sweep circuits discussed below.

If gated operation is not desired, a switch (not shown) removes the Gate input and provides grid 3 of the mixer with zero bias. In this event the circuit produces a

Fig 11.

MIXER CIRCUIT

Resistors are given in ohms unless marked K for thousands or M for megohms. Resistor ratings are ½ watt.

Condenser values are in microfarads. Polarity marks indicate electrolytic condensers.

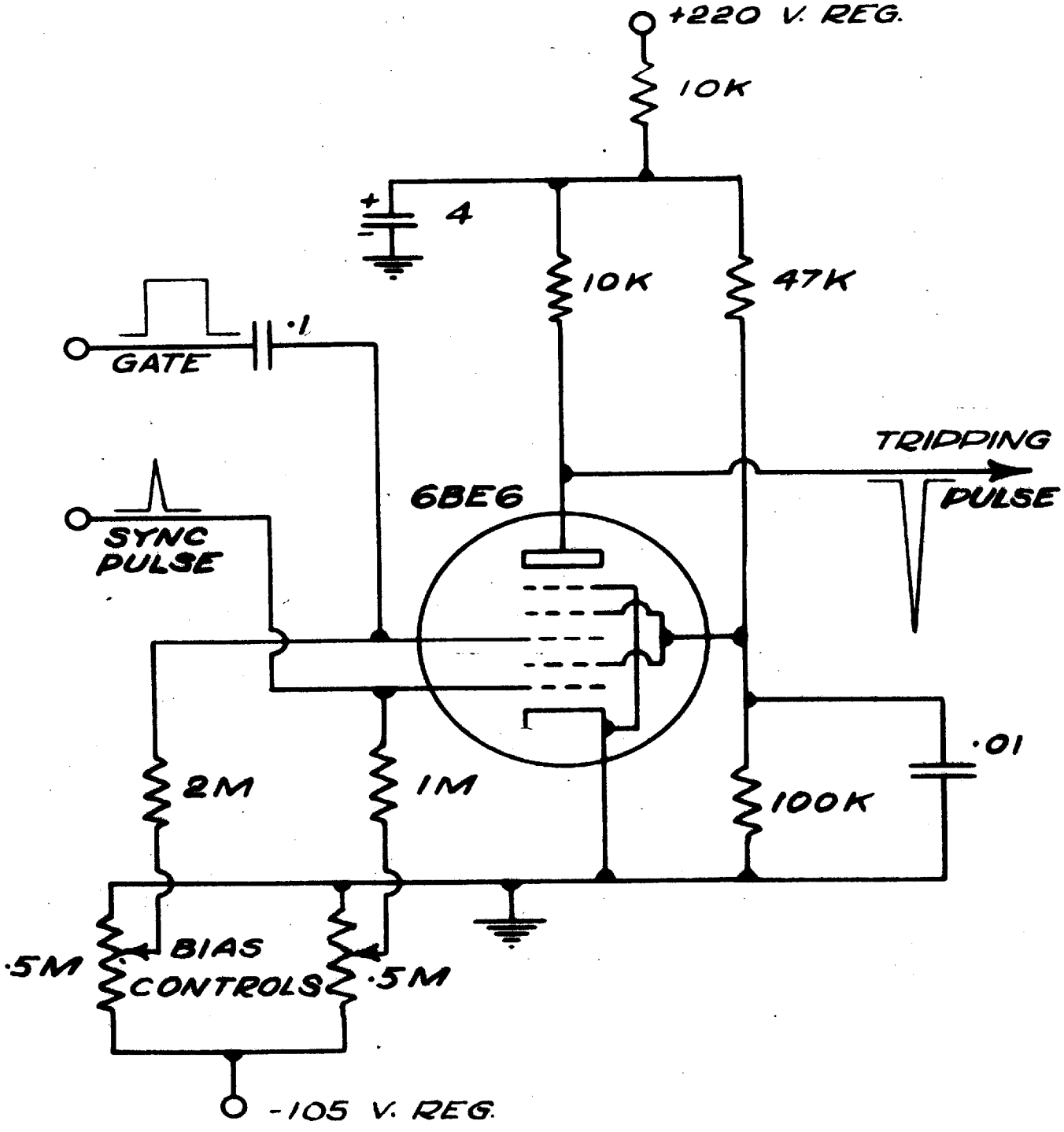
+220 V. REG.
10K
4
10K
47K
.1
GATE
TRIPPING
PULSE
6BE6
SYNC
PULSE
.01
2M
1M
100K
.5M
BIAS
CONTROLS
.5M
-105 V. REG.

Tripping Pulse for each synchronizing signal entering the Synchronizing Pulse Amplifier.

11. Beam Pulse Generator. The purpose of this circuit is to generate a pulse of voltage suitable for brightening the Cathode Ray beams when a signal is to be displayed on the screens, so that at other times the screens may remain dark. The essential requirements for such a pulse are that it be flat topped and have a rapid time rise. It should also commence as soon as possible after the beginning of the tripping pulse, so that the beginning of the signal to be studied will not be obscured.

The heart of the circuit is the single shot multivibrator consisting of tubes T1 and T2 in Fig 12. Since the grid of the pentode T1 is returned to B+, this tube is normally conducting, and its screen is normally at +68 volts. A voltage divider between the screen and the -105 volt supply couples to the grid of T2 which is normally slightly below cutoff at -9 volts. A 10 picofarad pulse sharpening condenser is also used from screen to grid. Screen coupling was used in preference to plate coupling to avoid undue loading of the pentode plate circuit. The result on tripping the multivibrator is a rapid rise to B+ in the pentode plate voltage.

The Tripping Pulse from the Mixer (Fig 11) is applied to the grid of the pentode through a small condenser. The critical pulse height for tripping, or sensitivity, is

Fig 12.

BEAM PULSE GENERATOR CIRCUIT

Resistors are given in ohms unless marked K for thousands or M for megohms. Resistor ratings are ½ watt unless otherwise specified.

Condenser values are given in <u>picofarads</u> unless marked uF for microfarads. Polarity marks indicate electrolytic condensers.

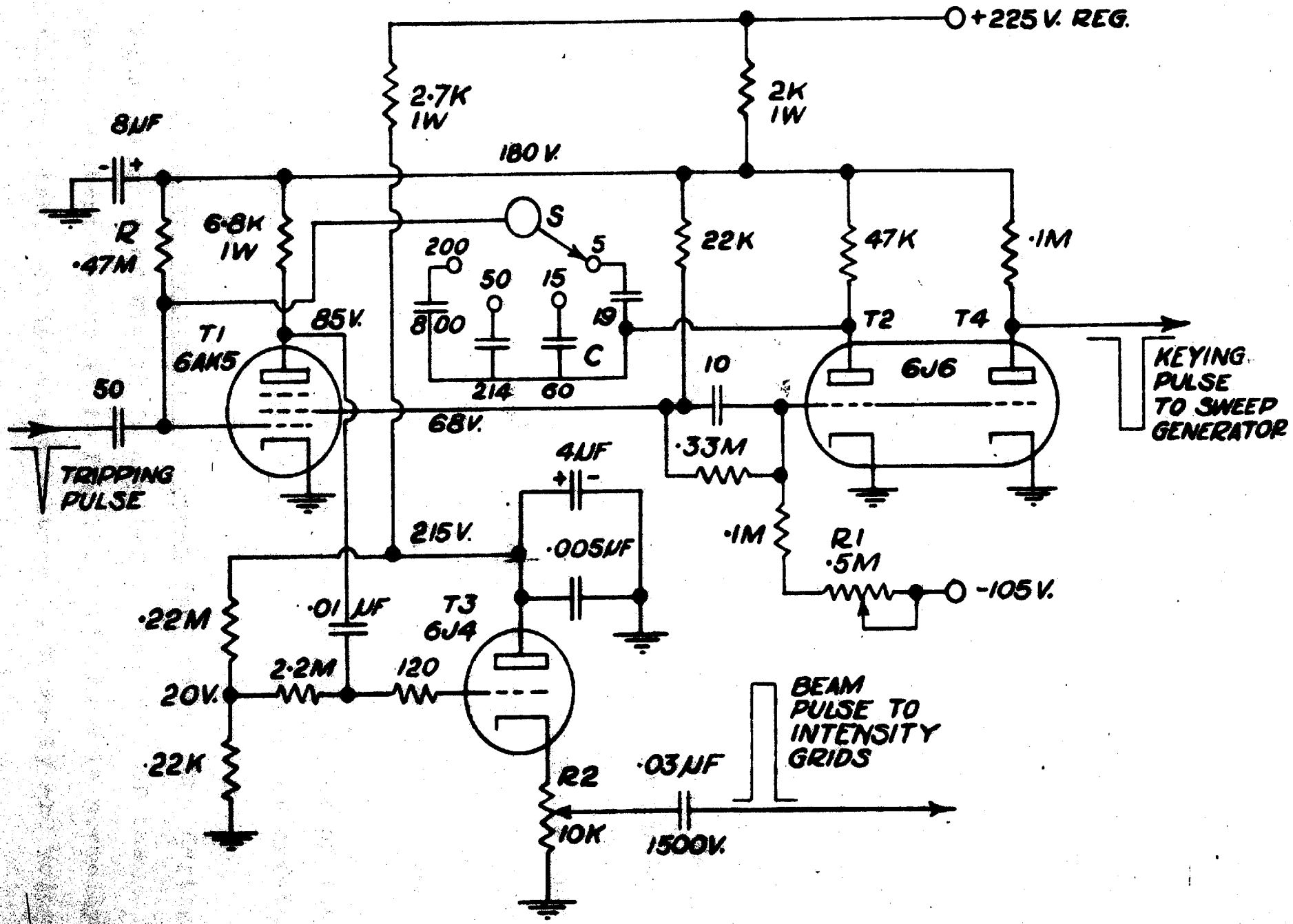
+225 V. REG.
2·7K 1W
2K 1W
180 V.
8 µF
R ·47M
6·8K 1W
S
200
50
15
5
8 00
19
C
214
60
22K
47K
·1M
T1 6AK5
85 V.
T2
T4
6J6
KEYING PULSE TO SWEEP GENERATOR
50
TRIPPING PULSE
68 V.
10
·33M
4 µF
·005 µF
215 V.
·1M
R1 ·5M
-105 V.
·22M
·01 µF
T3 6J4
2·2M
120
20 V.
·22K
R2 10K
·03 µF
1500 V.
BEAM PULSE TO INTENSITY GRIDS

adjustable, being controlled by R1. Upon the receipt of a negative pulse of sufficient size on the pentode grid, a rapid tripping action transfers conduction to T2. The grid of T2 is held at zero bias by the now increased screen voltage and voltage divider mentioned above. The grid of T1 is driven negative by the drop in plate voltage of T2 and coupling condenser C. When the pentode grid voltage has returned to cutoff by means of the RC decay circuit, conduction is resumed by T1.

The duration of the positive pulse generated at the plate of T1 is controlled by the time constant RC. Various values of C are selected by the switch S providing pulse lengths of 5, 15, 50 and 200 microseconds. This pulse is coupled to the grid of cathode follower T3, with the Contrast Gain Control R2 as its cathode load. The Beam Pulse output of R2 is applied to the intensity grids of the cathode ray tubes through a suitable blocking condenser for beam brightening.

T4 is used to produce a negative Keying Pulse of the same duration as the Beam Pulse for the purpose of driving the Sweep Generator.

12. Sweep Generator and Sweep Amplifier. The Keying Pulse from T4 of Fig 12 is applied to the grid of the sweep generator tube T1 in Fig 13. This tube is normally at zero bias, and its plate voltage is normally +10 volts.

Fig 13.

SWEEP GENERATOR AND AMPLIFIER CIRCUIT

Resistors are given in ohms unless marked K for thousands or M for megohms. Resistor ratings are ½ watt unless otherwise specified.

Condenser values are given in microfarads unless marked PF for picofarads. Polarity marks indicate electrolytic condensers.

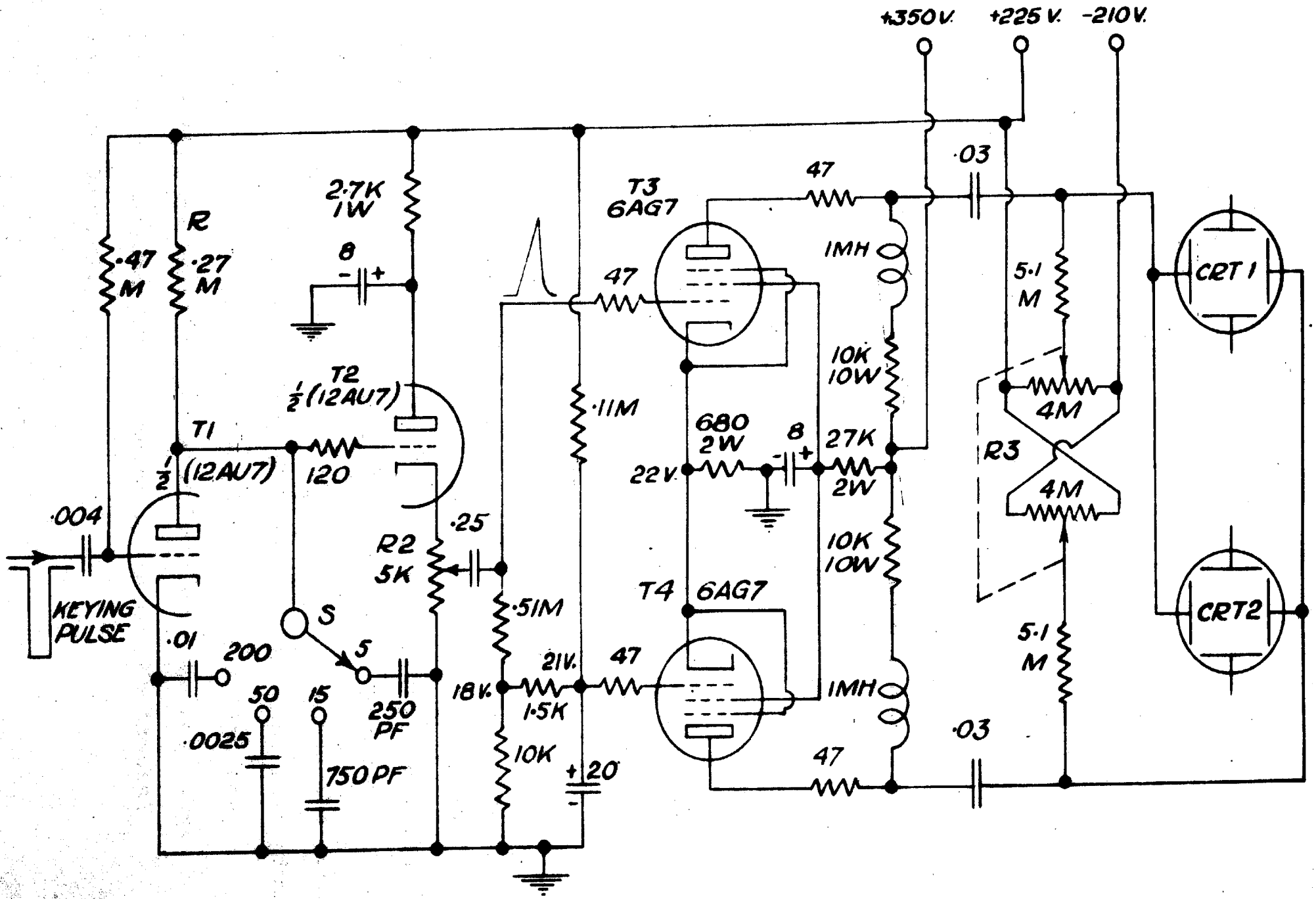
+350V.
+225 V.
-210V.
.03
47
T3
6AG7
1MH
47
5.1
M
CRT 1
10K
10W
4M
R3
4M
680
2W
8
27K
2W
22V.
10K
10W
T4
6AG7
5.1
M
CRT2
1MH
47
.03
47
2.7K
1W
8
R
.47
M
.27
M
T2
½(12AU7)
T1
½(12AU7)
120
.11M
.004
.25
R2
5K
.51M
KEYING
PULSE
.01
200
S
5
50
15
.0025
750 PF
250
PF
18V.
21V.
1.5K
10K
+20
-

If C is the Capacity connected between the plate and ground, then the plate voltage E will rise when the grid is driven beyond cutoff by the Keying Pulse, the instantaneous plate voltage t seconds after cutoff being given by the equation

$$E = (E_b - E_1)(1 - e^{-\frac{t}{RC}}) + E_1 \qquad (3)$$

where E_1 is the initial plate voltage, E_b is the plate supply voltage, and R is the plate load resistance. At the conclusion of the Keying Pulse, C is discharged through the tube, the plate voltage rapidly returning to its initial value E_1.

Switch S provides the selection of various values of C to correspond with different Beam Pulse durations. The C values chosen give about 15 volts of rise in E between the beginning and end of the Beam Pulse. Since this is only about 7% of $(E_b - E_1)$, the voltage rise is approximately linear with time in the interval. This sweep voltage is applied directly to the grid of T2, a cathode follower having the Horizontal Gain control R2 as its cathode load. The output contact of R2 is fed to the push-pull sweep amplifier, tubes T3 and T4. The amplifier gives uniform response up to one megacycle, and drives the horizontal deflecting plates of both cathode ray tubes. The dual 4 megohm potentiometer R3 is the Horizontal Position Control.

A switch (not shown) permits the selection of a continuous 60 cycle sawtooth sweep voltage as the input to T2. This sawtooth voltage is synchronized with the line frequency, and is generated by a conventional relaxation oscillator circuit using a thyratron.

13. Power Supplies. The various power supplies shown in the right hand column of Fig 4 are powered from the Model 1000 Sorensen Regulator at the bottom. Space prohibits the discussion of these in detail, but a summary will be made here. Critical voltages were provided by electronic regulators of the type described by Hill[9], and the operation and method of adjusting these is given in the appendix.

The Main Power Supply provides +350 volts unregulated DC at 30 milliamperes for the Sweep Amplifier, +225 volts regulated DC at 70 milliamperes and -105 volts DC (VR tube regulated) for the pulse and sweep generators, -210 volts DC (VR tube regulated) for the position controls, and 6 volts AC for the heaters.

The Accelerator Power Supply provides -1500 volts DC for the cathodes and 6 volts AC for the heaters of the cathode ray tubes.

The Intensifier Power Supply provides +10 kilovolts DC for the intensifier electrodes of the cathode ray tubes. It is an RF type Dumont High Voltage Power Supply, Model 263A. The above three supplies were combined in one

chassis for convenience.

The Video Power Supply provides 650 volts unregulated DC at ½ amp for the finals, and 220 volts regulated DC at 150 milliamperes for the remaining stages of both Video Amplifiers. 6 volts AC is also provided for the heaters of the video amplifier tubes.

The Phototube Power Supply provides 220 volts regulated DC at 15 milliamperes, and 6 volts AC for the cathode follower of the Phototube Unit, and a maximum of -1200 volts regulated DC at 1.2 milliamperes for the multiplier phototube. The 1200 volt regulator is of the type used by Kessler and Wolfe[10] for the same purpose, and is provided with a manual voltage control providing a range of 20 to 120 volts per stage on the phototube.

14. Marker and Square Wave Generator. This unit provides a source of 100 kilocycle square waves used as described above in section B.9. By differentiating the square wave output, marking pulses are generated at five microsecond intervals having alternate polarity.

The circuit is shown in Fig 14. T1 is a relaxation oscillator arranged to produce at A, a short positive pulse at a repetition rate of about 500 per second. This pulse is used as the synchronizing output, and also trips the gate tube T2 which generates at B a 250 microsecond negative gate. This gate is applied to the grids of the keying tube T3 which drives it quickly to cutoff causing shock oscil-

Fig 14.

MARKER AND SQUARE WAVE GENERATOR CIRCUIT

Resistor values are given in ohms unless marked K for thousands or M for megohms. Resistor ratings are ½ watt unless otherwise specified.

Condenser values are in microfarads unless marked PF for picofarads. Polarity marks indicate electrolytic condensers.

Inductances are in microhenries except where marked MH for millihenries. L1 is a parasitic suppressor. L2 is a slug tuned peaking coil.

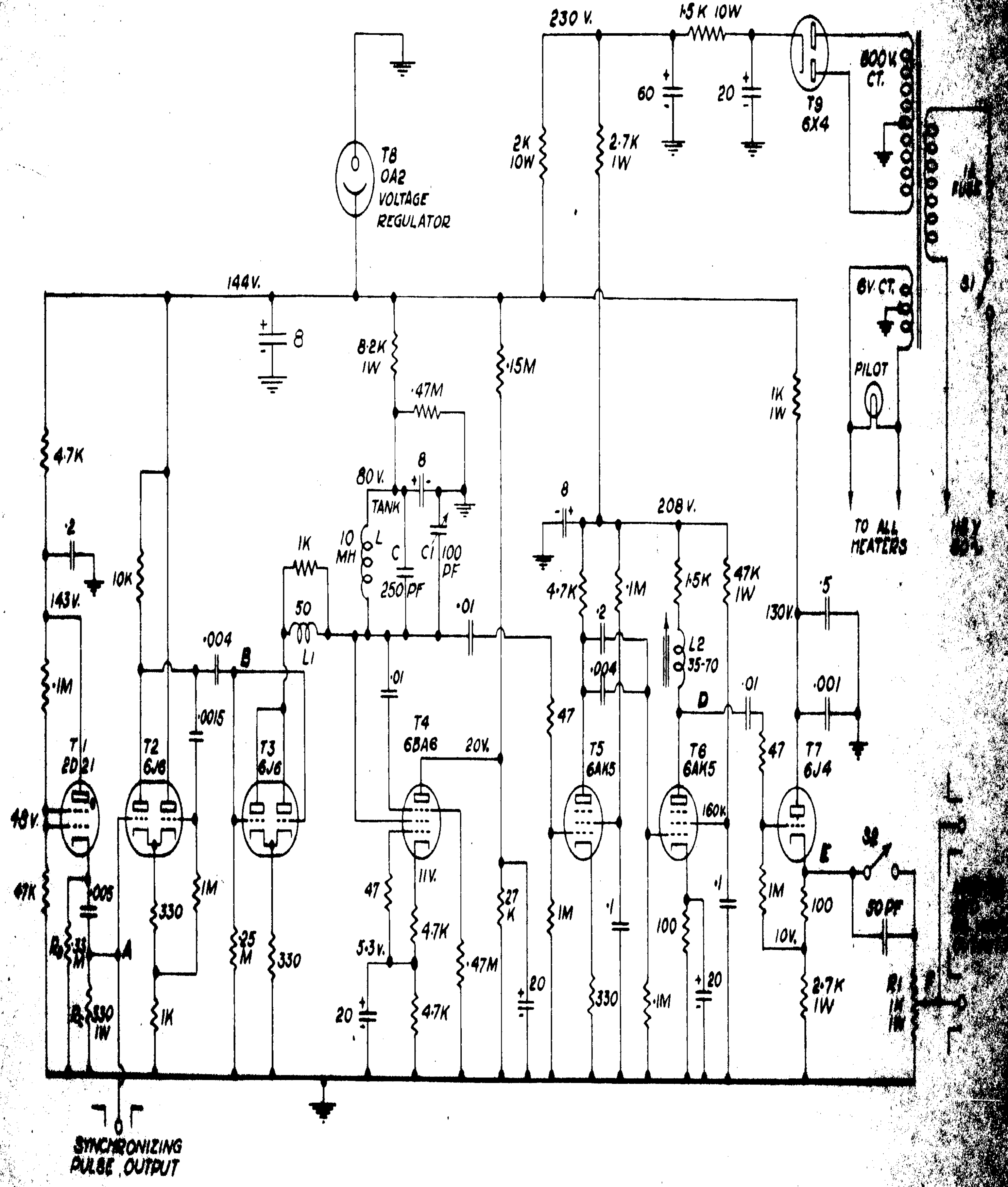
230 V.
1·5 K 10W
60
20
T9
6X4
800 V.
CT.
2K
10W
2·7K
1W
T8
OA2
VOLTAGE
REGULATOR
144 V.
8
8·2K
1W
·47M
·15M
6V. CT.
PILOT
1K
1W
4·7K
80 V.
8
TANK
10
MH
L
C
250 PF
C1
100
PF
·2
143 V.
10K
1K
50
L1
·01
8
208 V.
4·7K
·1M
1·5K
47K
1W
130V.
·5
TO ALL
HEATERS
·1M
·004
B
·0015
·01
T4
6BA6
20V.
·2
·004
L2
35-70
D
·01
·001
47
47
T1
2D21
T2
6J6
T3
6J6
T5
6AK5
T6
6AK5
160K
T7
6J4
48V.
47K
·005
1M
11V.
E
47
4·7K
27
K
1M
·1
100
·1
1M
100
50 PF
10V.
330
·25
M
330
A
5·3 V.
4·7K
·47M
20
20
330
·1M
20
2·7K
1W
1K
330
1W
20
4·7K
R1
1K
1W
SYNCHRONIZING
PULSE OUTPUT

lation of the LC tank circuit. Transitron oscillator T4 sustains the oscillations in the tank at approximately constant amplitude for the duration of the gate. At the conclusion of the gate, the keying tube resumes conduction, and damps out the tank oscillations by virtue of its low plate resistance.

Trimmer condenser C1 was adjusted to produce an oscillator frequency of 100 kilocycles $\pm$ ½%. This was done by oscilloscopic comparison with the output of a Hewlitt Packard oscillator generating 50 kilocycles. The latter was previously calibrated against the WWV frequency standard. The T4 oscillator operates by virtue of the negative resistance offered by its screen to the tank circuit. It is stabilized in frequency by supplying the circuit with regulated B+ voltage from the voltage regulator tube T8.

T5 and T6 are clipper stages which convert the oscillator output into a square wave at D. The peaking inductance L2 was adjusted to give an output wave having minimum time rise without overshoot. The cathode follower T7 provides low output impedance.

When switch S2 is open, the output E of the cathode follower is differentiated by an RC circuit having a time constant of .05 microseconds. The output wave produced at F is then a series of marking pulses of alternate polarity

spaced at 5 microsecond intervals. When S2 is closed, the square wave output is obtained. R1 is the output gain control for both markers and square waves.

A train of pulses is initiated by the trigger pulse at A, the train lasting for about 250 microseconds, and these trains are repeated at a 500 cycle rate.

Rise time of a pulse is usually expressed as the time taken in going from 10% to 90% of maximum value. On this basis, the rise time of the square wave output was slightly less than 0.1 microsecond as indicated by a synchroscope having a calibrated one microsecond sweep.

C. SUMMARY OF DUOSCOPE OPERATION

1. The various units discussed act together as diagrammed in Fig 4. When a synchronizing input signal is received during the Gate, the Mixer transmits a negative Tripping Pulse to the Beam Pulse Generator. The beams of the two cathode ray tubes are brightened, and the driven sweep initiated. Whatever signals are applied to the inputs of the two Video Amplifiers are then displayed on the cathode ray screens for the duration of the sweep. Sweep duration is controlled by a switch S in the Beam Pulse Generator circuit, Fig 12. Driven sweeps of 5, 15, 50 and 200 microseconds are provided. Sweep calibration may be obtained by applying the 5 microsecond marking pulses from the Marker

Generator to the input terminals of one or both Video Amplifiers.

2. Synchronizing Signal. Since a large burst of electromagnetic energy is released from the spark source at the beginning of each spark, a few feet of wire acting as an antenna pickup provides an adequate synchronizing signal. Because of the full wave rectifier feature of the Synchronizing Pulse Amplifier, the beginning of the first oscillation (whether positive or negative) of antenna voltage generates the required Tripping Pulse when it coincides with the Gate.

3. Adjustment of the Gate. When it is desired to observe only one signal of several which may occur during the cycle, signals are displayed on a 60 cycle sweep. When using this sweep, a portion of the Gate is fed to the intensity grids of the cathode ray tubes. Thus a portion of the trace is brightened, permitting the Gate phase position to be observed and adjusted to include the signal desired. The Gate width is also adjustable, and must be narrow enough to permit only the signal desired to be selected, yet wide enough to take account of the time jitter of this signal.

After the Gate width and phase are adjusted, driven sweep operation is selected, and the desired signal displayed on a suitable fast sweep. Either manual or

continuous gating may be employed, the latter being most useful for visual observation. In photographic recording, manual gating is used to obtain single-shot exposures, and the intensity controls are adjusted to keep the screens dark when no signals are displayed.

To obtain a film record of the whole sequence of events, ungated operation may be used as described at the bottom of Page 30. In this case the sweep is initiated for each spark, and the film is moved sufficiently between sparks to separate the images.

III. PHOTOTUBE CHARACTERISTICS

A. Circuit for Maximum Gain

Since the problem of shielding the signal cables against the high frequency electromagnetic field of the spark source is less serious as the signal level is raised, it is desirable to obtain the maximum gain from the phototube commensurate with the bandwidth required. The frequency response of the Phototube Unit will fall with increasing frequency to 70% when a frequency f_o is reached such that

$$2\pi f_o CR = 1 \qquad (4)$$

where C is the shunting capacity in farads in the output circuit of the phototube, and R is the anode load or coupling resistance in ohms. It is desired to examine frequency components up to 10 megacycles if possible, and by substituting $f_o = 10^7$ and $C = 10^{-11}$ farads in equation (4), a value R = 1600 ohms is obtained. This value was used as the anode load of the phototube as shown in Fig 3.

B. Noise and Dark Current.

The root mean square noise voltage due to dark current in a nine stage multiplier phototube is given by the equation[10]

$$\overline{V_f^2} = 2R^2 e \, \Delta f I_o \frac{x^{10} + 1}{x + 1} \qquad (5)$$

where $\overline{V_f}$ is the RMS noise voltage between f and f + Δf cycles per second, R is the anode load resistance in ohms, e the electronic charge, I_o the DC component of dark current, and x the mean stage gain of the phototube dynodes.

Measurements on early models of 1P28 phototubes gave dark currents of the order of 10^{-7} amperes. Recent improvements in construction of these tubes have resulted in considerably reduced dark currents. Twelve new 1P28 phototubes were tested at 100 volts per stage. Of these one was unstable (gas reject) and another had a dark current of 22 x 10^{-9} amperes. Dark currents of the remaining ten tubes ranged from 0.8 to 9.2 x 10^{-9} amperes, the average being about 2 x 10^{-9} amperes. Using this average value in equation (5) and assuming a total amplification of x^9 = 200,000 one has $\overline{V_f}$ = 5 x 10^{-5} RMS volts with R = 1600 ohms and a 10 megacycle bandwidth.

Since this voltage is well below the detectability of the Duoscope at full gain, no noise fluctuations would be expected to appear on the oscilloscope screen in the absence of signal, and this was indeed the case.

C. Noise and Signal Current

If the photocurrent at the cathode is i_p, then the output current due to the light is

$$I_p = ui_p \tag{6}$$

where u is the amplification of the phototube. Anode noise current due to shot effect from the photoelectrons will be produced, the RMS output current being

$$(\overline{I^2})^{\frac{1}{2}} = u(2e\Delta f i_p)^{\frac{1}{2}} \tag{7}$$

To this the RMS noise due to the dark current must be added, but this has been shown to be so small for the new tubes that it may be neglected here. The signal to noise ratio S may now be found by dividing (6) by (7) resulting in the equation

$$S^2 = \frac{u^2 i_p^2}{u^2 2e\Delta f i_p} = \frac{i_p}{2e\Delta f} \tag{8}$$

For an output current of one milliampere, and an assumed amplification of 200,000 one obtains S = 39 for the theoretical signal to noise ratio at a 10 megacycle bandwidth. In practice a slightly smaller S is obtained because of the random process of secondary emission not taken into account in equation (7).

Equation (8) shows the significant fact that S is independent of the values of u and the load resistance R. It also shows that only two methods are available for

increasing S. The first is by decreasing the bandwidth Δf, and the second is by increasing the photocathode current i_p.

A consequence of decreasing the bandwidth is loss of detail in the signal being observed, but since this detail may be obscured anyway by the noise fluctuations, an optimum value of bandwidth will exist for each signal, depending upon the amount of noise which may be tolerated and the character of the signal itself. For this reason a bandwidth control is provided in the circuit of Fig 3.

D. Selection of Phototubes

The significance of obtaining the largest possible value of i_p is that we require the most sensitive photosurface available. Twelve 1P28 phototubes were therefore tested for sensitivity, and for this purpose a reproducible light pulse generator was constructed. This consisted of a ¼ watt neon tube in a relaxation oscillator circuit operated from a controlled voltage source, the neon tube producing light pulses of about 50 microseconds duration, and of uniform peak intensity. The results of testing the twelve tubes at 100 volts per stage were peak anode currents ranging from 25 to 4400 microamperes, with an "average" tube giving about 200 microamperes. The most sensitive tube, which was selected for subsequent work, was thus about 20 times as sensitive as an average tube.

A further consequence of obtaining a large i_p is that the maximum amount of light available must be used. The strongest spectral lines available were therefore chosen, and the entrance and exit slits on the spectrograph made as large as was commensurate with proper spectral line isolation. On occasion a quartz lens was used to form an image of the sample gap on the spectrograph collimating lens, but this could not be used in the fluctuation studies since variations in spark position on the electrodes introduced an abnormal amount of fluctuation in light received by the phototube.

E. Fatigue in Phototubes

Large photocurrents are known to produce fatigue in multiplier phototubes, the rate of fatigue being approximately proportional to the intensity of illumination[11].

As will be shown later, the effect of fatigue is of but secondary importance in the present study. It should also be mentioned that fatigue in a multiplier phototube is due chiefly to loss of sensitivity of the later dynode surfaces, and therefore a large photocathode current i_p which is desirable for the reasons outlined above, need not necessarily result in bad fatigue effects provided the tube gain is reduced by lowering the dynode potentials.

F. Methods of Attenuation

Let it be assumed that sufficient light and tube sensitivity are obtainable to produce more than adequate signal voltages for recording the intensity patterns. It then becomes necessary to choose between three methods of attenuation:

(a) decrease the amplifier gain,

(b) decrease the phototube gain by reducing the dynode potentials, or

(c) decrease the light intensity falling on the phototube with the aid of neutral filters[10] or by reducing the areas of the entry and exit slits of the spectrograph.

Method (c) must be avoided since it decreases i_p with a resulting loss in signal to noise ratio. Since no loss in this ratio results from either (a) or (b), the choice is based on reduction of tube fatigue. Since this was accomplished by method (b) a phototube voltage control was mounted on the front panel of the Phototube Power Supply, and this was used as the gain control for the system.

IV. THE SPARK SOURCE

A. CIRCUIT AND OPERATION

1. General. For suitable spark excitation, relatively high peak currents and high discharge voltages are required. The method commonly employed is to build up a high voltage in a condenser bank and discharge the stored energy quickly through the sample gap.

In the Air Interrupted Spark Source circuit Fig 15, a variac T1 is used to control E_o the input voltage to the primary circuit. T2 is a 25 KVA transformer, and R_o is inserted in series with the primary to limit the current. The secondary, rated at 33,000 volts, charges condenser C through R_3 to a voltage E_{pk} at which time the discharge circuit operates by the breakdown of the gaps G_1 and G_2.

A variable inductance L_1 and a variable resistance R_1 are used to control the spark current. An oscilloscope is commonly employed to observe the break pattern and measure the breakdown voltage E_{pk} on condenser C. For this purpose a suitable condenser divider must be employed. The peak spark current I_{pk} may be measured with an oscilloscope connected across the non inductive resistance R_2 described in Chapter II, provided certain precautions in impedance matching and frequency response are observed.

Fig 15

SIMPLIFIED CIRCUIT OF THE

AIR INTERRUPTED SPARK SOURCE

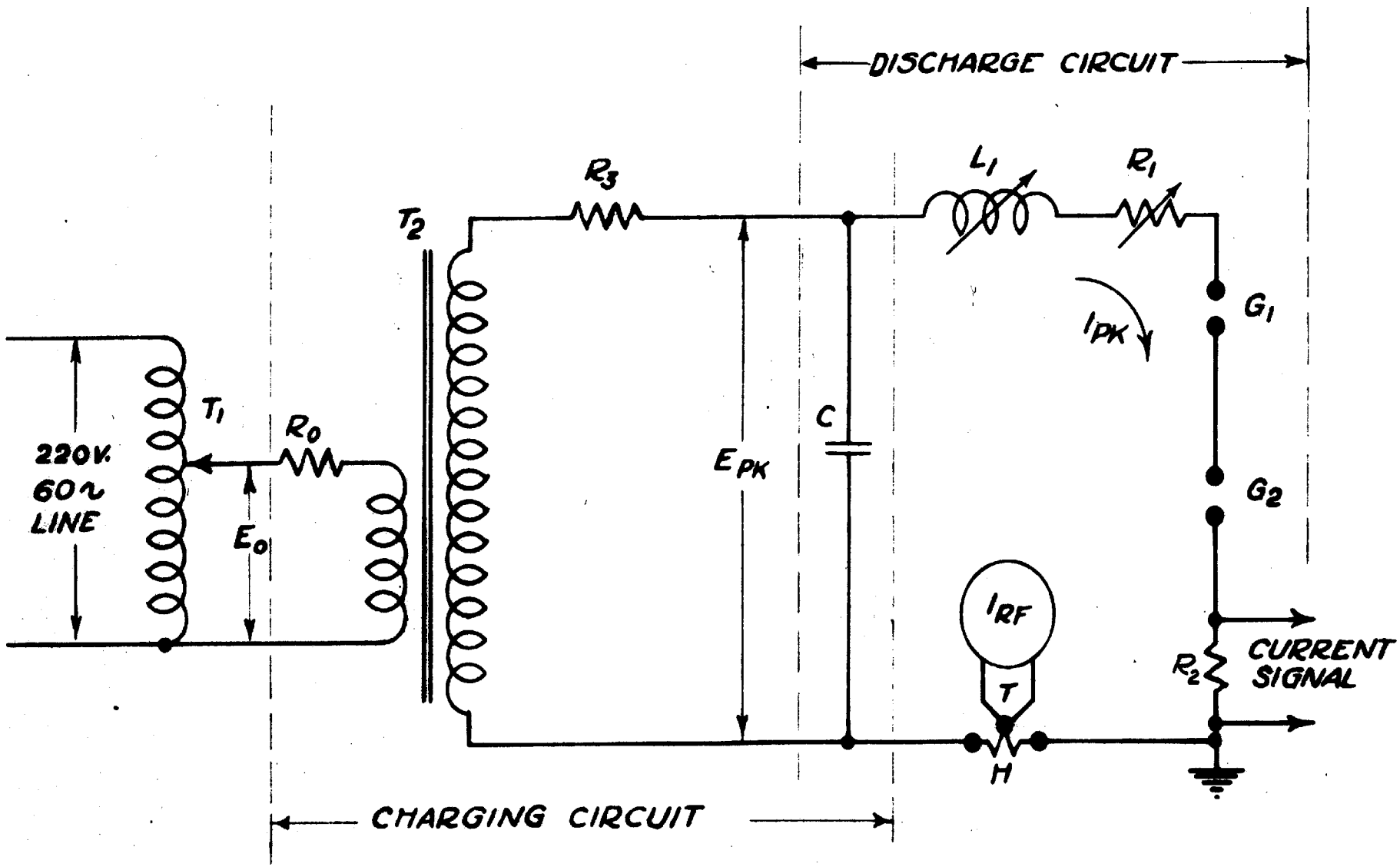
DISCHARGE CIRCUIT
R_3
L_1
R_1
T_2
G_1
I_{PK}
T_1
R_0
220V. 60~ LINE
E_0
E_{PK}
C
G_2
I_{RF}
T
R_2
CURRENT SIGNAL
H
CHARGING CIRCUIT

The RMS radiofrequency current in the discharge circuit may be measured with a thermocouple type ammeter, the thermal junction T and low resistance heater H placed in the circuit as shown.

2. Charging Cycle. The operation of the Air Interrupted Spark Source is discussed by Enns and Wolfe[12], the charging and discharge cycles being considered separately. It is general practice at present to use non-resonant charging of the condenser by making R_o and R_3 large enough to produce critical damping of the charging transient. If a small charging time constant is used, the condenser voltage may reach E_{pk} several times in a half cycle of line frequency, thus producing several sparks per half cycle. The number depends upon the charging time constant and the input voltage E_o to the charging circuit. It may range from one to thirty or more sparks per half cycle.

3. Discharge Cycle. The breakdown voltage E_{pk} is controlled by the spacing of the control gap G_1, and is substantially constant for a given spacing. Since each spark removes nearly all the energy stored in the condenser, approximately equal amounts of energy are delivered. Energies commonly employed in this work range from 0.2 to 10 joules per spark. This energy is shared between the gaps and ohmic resistance in the discharge circuit.

The control gap G_1 is centred in a non turbulent stream of air having a velocity of about 100 meters per second. The air stream quickly removes ionized gases from the electrodes after each spark, producing an open circuit. The velocity of the air stream is somewhat critical. If it is too high, the arcing voltage across G_1 appears to rise somewhat toward the end of the discharge period, producing undesirable variations in the energy division between the gaps. If it is too low, the ions are not cleared away rapidly enough, and this results in an erratic breakdown voltage.

B. Nature of Spark Discharge

1. For each spark an underdamped oscillatory current flows in the discharge circuit. If R is the total ohmic resistance, L the total series inductance, and C the capacity in the circuit, the discharge frequency F is given by

$$w = 2\pi F = \sqrt{\frac{1}{LC} - \frac{R^2}{4L^2}} \cong \frac{1}{\sqrt{LC}} \qquad (9)$$

The approximation holds within 1% if $R < .28\sqrt{\frac{L}{C}}$, which is generally the case for normal operating conditions.

If V, the sum of the arc drops across the gaps is assumed constant over the first half cycle of discharge current, a simple equivalent circuit may be drawn for this interval. From this one may obtain the condenser

voltage as a function of time, thus

$$E = V + (E_{pk} - V)\, e^{-\frac{R}{2L}t} \cos wt; \quad 0 \leq wt \leq \pi \qquad (10)$$

where E_{pk} is the initial value of E, and w is defined by equation (9).

The difference d in magnitude of condenser voltage between the beginning and end of the half cycle is found by substituting wt = 0, π in equation (10), and subtracting the absolute values:

$$\begin{aligned} d &= |E_o| - |E_\pi| \\ &= |E_{pk}| - \left|V + (E_{pk} - V)e^{-\frac{R}{4LF}} \cos \pi\right| \\ &= |E_{pk}| \cdot (1 - e^{-\frac{R}{4LF}}) + |V| \cdot (1 + e^{-\frac{R}{4LF}}). \end{aligned} \qquad (11)$$

As $R \to 0$, $d \to 2V$, and the envelope of the condenser voltage wave approaches a straight line since equal increments of voltage, 2V are lost each half cycle. The loss per cycle is therefore 4V, and p, the number of oscillations in the discharge may now be calculated by the equation

$$p = \frac{|E_{pk}| - |E_r|}{4V}; \quad R = 0 \qquad (12)$$

where E_r is the voltage remaining on the condenser at the end of the discharge period.

The discharge current I, may be obtained for the first half cycle by differentiating equation (10) and multiplying by the capacity C:

$$I = C\frac{dE}{dt}$$

$$= C\,(E_{pk} - V)\left\{\frac{-R}{2L}\,e^{-\frac{R}{2L}t}\cos wt - we^{-\frac{R}{2L}t}\sin wt\right\}$$

$$0 \leqslant wt \leqslant \pi \qquad (13)$$

As $R \rightarrow 0$ this becomes

$$I = -(E_{pk} - V)\sqrt{\frac{C}{L}}\sin wt; \qquad \begin{matrix} R = 0 \\ 0 \leqslant wt \leqslant \pi \end{matrix} \qquad (14)$$

and the peak current occuring at $wt = \frac{1}{2}\pi$ has the value

$$I_{pk} = \sqrt{\frac{C}{L}}\,(E_{pk} - V); \qquad R = 0 \qquad (15)$$

Further details regarding the nature of spark discharges may be found in the work of Kaiser and Wallraff[13] and others[14, 15].

2. Fig 16 shows A the condenser voltage, and B the spark current waves on a horizontal time axis. As mentioned above, a residual voltage is left on the condenser at the end of the discharge period. This voltage is either positive or negative as the discharge terminates at point P (solid line) or point Q (dotted line).

If the residual condenser voltage is positive, the time required to recharge the condenser to $+E_{pk}$ will be less than if it is negative. The voltage pattern alternates in a random way between these two conditions giving rise to a time jitter, or variation in firing time of the second and subsequent sparks in each half cycle. Slight

Fig 16.

VOLTAGE AND CURRENT WAVES IN THE DISCHARGE PERIOD

A. Condenser Voltage

B. Spark Current

C. Detail of B near zero

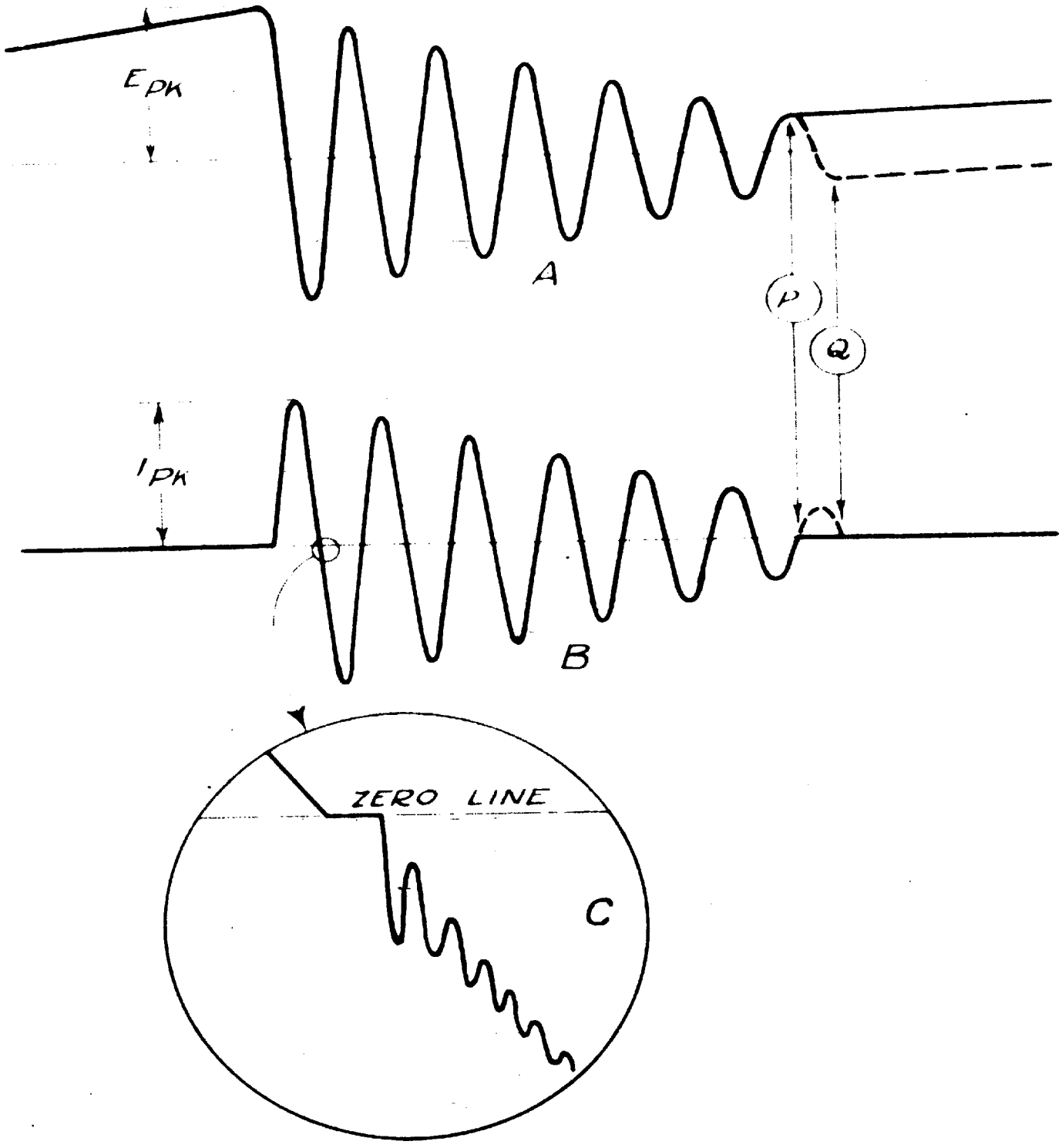
E_{PK}
A
P
Q
I_{PK}
B
ZERO LINE
C

variations in the breakdown voltage E_{pk} cause an additional time jitter. The jitter in later sparks in the half cycle is always larger than in early sparks since the effect is cumulative over each half cycle period. A time jitter of 500 microseconds is not uncommon for the last spark of a half cycle. This point must be considered in certain types of direct reading analyzers using tuned filters.

The fluctuation in p, the number of oscillations per spark, may be shown by a continuous film record of condenser voltage. A fast horizontal driven sweep, and slow vertical film motion are combined to facilitate comparison of the wave forms. A portion of the film record for 5 sparks per half cycle is shown in Fig 17. Time is increasing from top to bottom, and the portion of the record shown represents an interval of 1/15 second. Each separate oscillogram of condenser voltage is displayed on a horizontal sweep of 100 microseconds.

Five millimeter gap spacings were used here in both gaps, electrode materials being tungsten in the control gap and iron in the sample gap. It may be noted from the oscillograms that p varied from 10 to 13, and occasionally an increase in E_{pk} occurred for the first spark in the half cycle.

Fluctuations in p and E_{pk} are reduced when gap electrodes of low vaporization temperatures are used. For this

Fig 17.

FILM RECORD OF CONDENSER VOLTAGE WAVES

Source Data: L = 300 microhenries

C = .0045 microfarads

R_1 = 0

F = 0.15 megacycles

Sparks per $\frac{1}{2}$ cycle = 5

Control Gap = 5 mm Tungsten

Sample Gap = 5 mm Iron

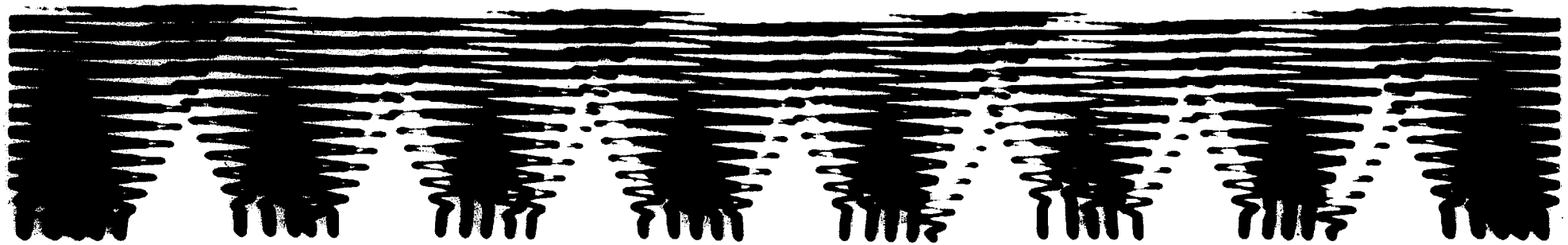

reason, magnesium electrodes[12] have been successfully employed in the control gap.

3. Parasitics. A close examination of the zeros in the current waves revealed the structure shown in C Fig 16. When the current reaches zero it remains there for a very short interval. This is the time required to charge the stray capacity associated with the gaps from their extinction voltage to an ignition voltage of opposite polarity. When the current is resumed, the abrupt current change gives rise to the damped parasitic oscillation shown. This was named the Re-ignition Parasitic because of its origin.

Parasitics are the result of shock oscillations of resonant circuits formed by stray capacities and inductances in the wiring of the source. One would then expect a parasitic at the beginning of the discharge, since a considerable shock is felt by the whole circuit when the spark first strikes. This Initial Parasitic is generally of greater amplitude and appears to contain more frequency components than the Re-ignition Parasitics, but it decays rapidly to a small value after a few microseconds. Parasitic frequencies ranging from one to thirty megacycles have been observed on different spark sources, but nothing has yet been proven about their effect on excitation.

Oscillograms in Fig 18 are for A condenser voltage, B spark current, and C current derivative waves for the first oscillation of the main discharge transient. Both Initial and Re-ignition Parasitics may be seen in the current wave B. The horizontal shelf at the current zeros is indicated clearly in the original record, but some of the detail is lost in the reproduction.

If a current shelf exists at the current zeros, the derivative of current, which is normally passing through a maximum value at these points should also return momentarily to zero. This return to zero appears in the points of wave C which correspond with current zeros. The derivative wave was obtained by inserting as a pickup, a small inductance (0.2 microhenry) in place of the resistance R_2 in Fig 14.

The current derivative of the main transient oscillation calculated here on the basis of measured peak current and frequency, has a maximum value of 38 amperes per microsecond. The peak value of current derivative observed in the region of the Re-ignition Parasitics was here greater than 200 amperes per microsecond. Thus although the parasitics appear quite small in the current wave, they take on a major role in the derivative wave when parasitic frequencies are high relative to the main transient frequency F.

Fig 18

OSCILLOGRAMS OF WAVES FOR THE FIRST OSCILLATION OF THE DISCHARGE PERIOD.

A. CONDENSER VOLTAGE

B. SPARK CURRENT

C. CURRENT DERIVATIVE

Source conditions:

E_o = 240 volts

R_o = 10 ohms

C = .034 microfarads

L = 280 microhenries

F = 50 kilocycles

R_1 = 2 ohms

R_2 = 1 ohm

E_{pk} = 12.7 kilovolts

I_{pk} = 117 amperes

Horizontal Sweep = 25 microseconds

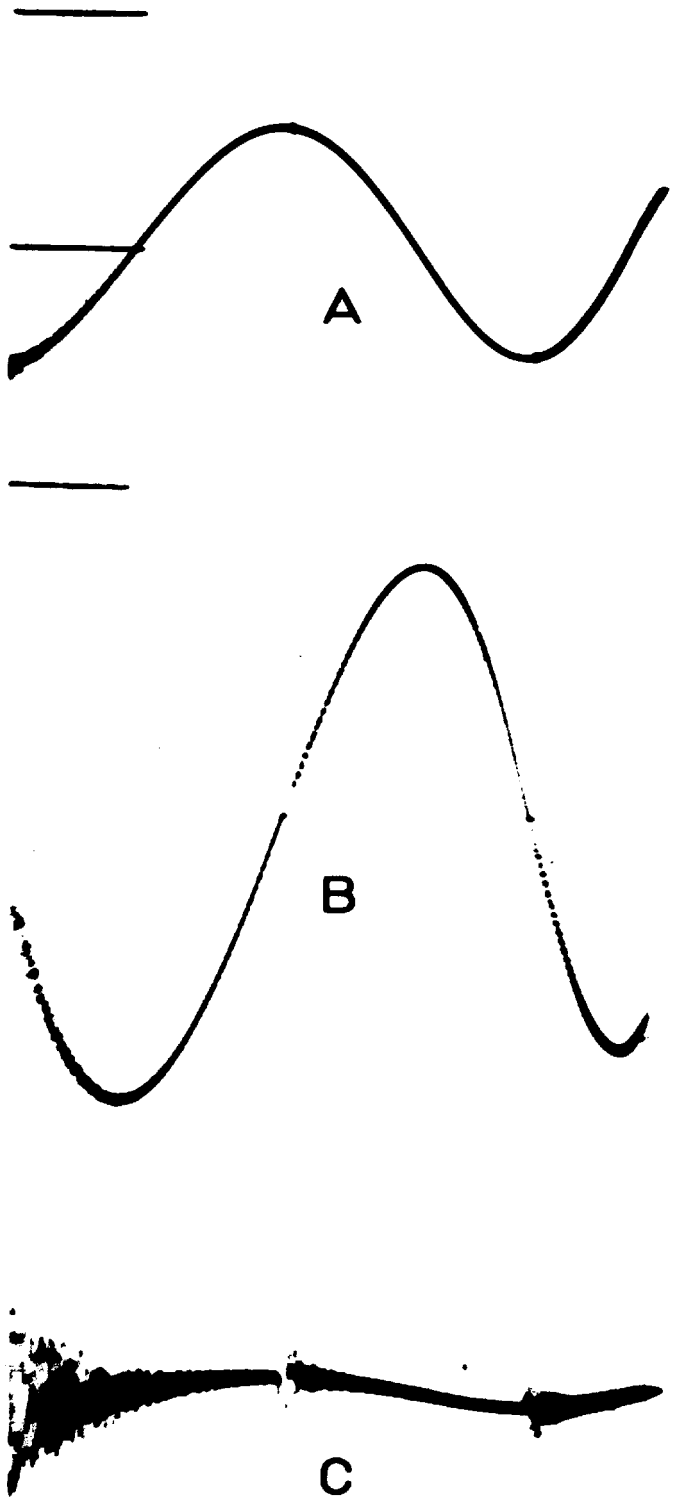
A
B
C

V. INTENSITY STRUCTURE OF SPECTRAL LIGHT

A. General

1. Ions and atoms may exist only in discrete energy levels as indicated by the familiar energy level diagram Fig 19. A transition from an upper to a lower level results in the release of a quantum of energy given off in the form of light.

Let us examine the possible course of an atom which has been doubly ionized by the removal of two of its valence electrons. This places it in the Double Ion Ground State A in the diagram. Its lifetime in this level will depend upon the availability of an electron for recombination. The double positive charge of the ion provides a strong force of attraction for any free electron in its vicinity, and the lifetime is fairly short if there are a number of free electrons present.

Once recombination begins, a cascade of transitions such as AB, BC, CD, DE results, and the ion now is found in the Single Ion Ground State E. During the cascade from A to E, each transition is accompanied by the emission of a spark line. For a particular spark line there is a particular transition between two levels, the upper level being termed the Origin of the line. For example, the spark line associated with the CD transition has the origin C.

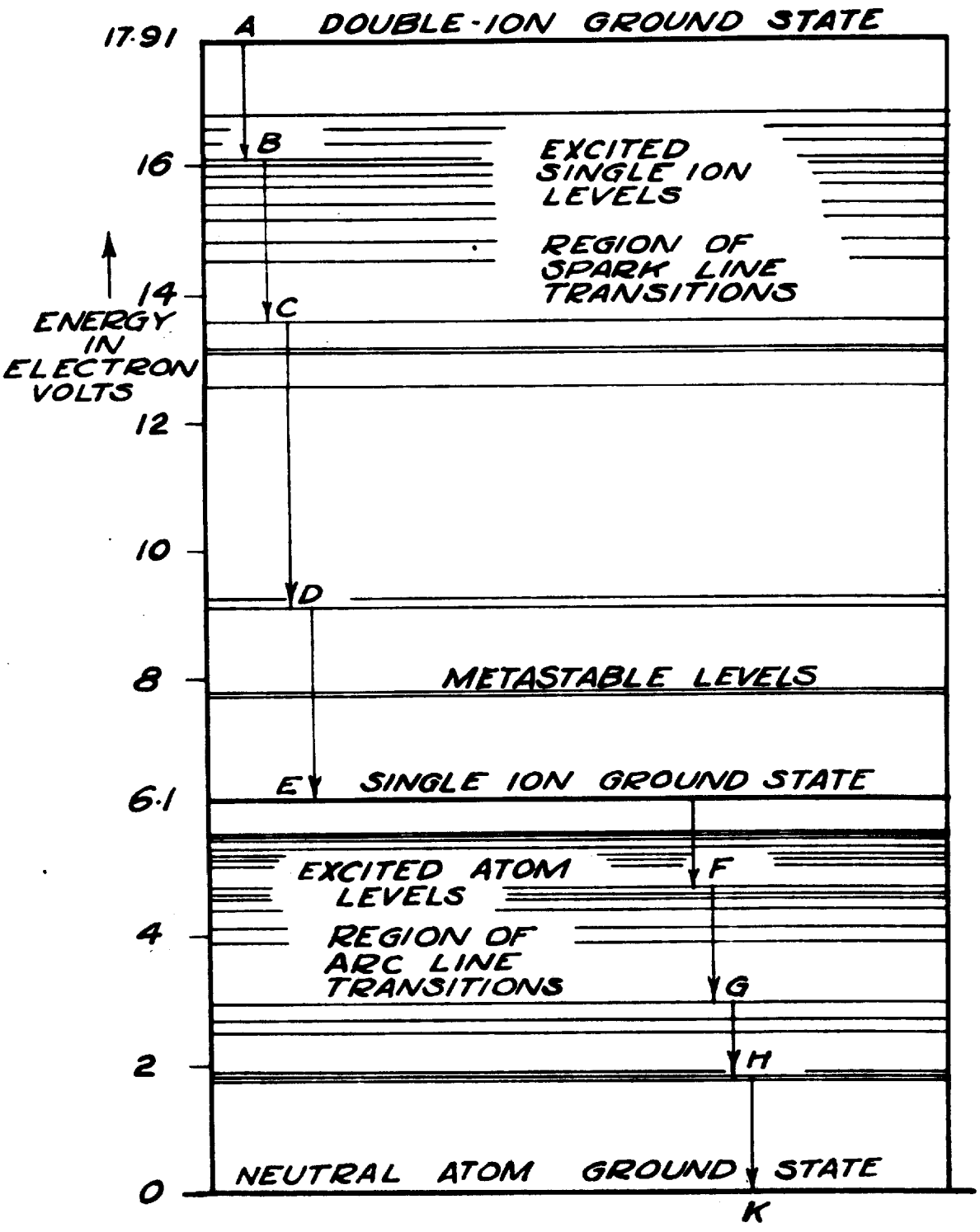

Fig 19. ENERGY LEVEL DIAGRAM

The lifetime in any intermediate level of the cascade is very short, about 10^{-8} seconds, and therefore all the spark lines are emitted in a very short time interval after the process of recombination begins. The probability of exciting the ion further during the cascade is quite small because of the short lifetime in any intermediate level, the only exception being in the case of metastable states. If an ion falls into a metastable level a downward transition is not permitted, and the only escape is through subsequent excitation to a higher level.

Upon reaching E, the lifetime will depend upon the availability of another electron for recombination. In this case the ion carrys only a single positive charge, giving only half the attractive force that it had in A. The lifetime is thus longer in E than in A for the same electron environment.

When an electron is captured however, a second cascade results, such as is illustrated by the transitions EF, FG, GH, HK. Each of these transitions is accompanied by the emission of an arc line, and the lifetime in any intermediate level is again very short, about 10^{-8} seconds. Again there is only a very small probability of disturbing the cascade by further excitation while in one of the intermediate levels.

2. In the spark source there exist two possible mechanisms of exciting the vapor particles to high energy levels.

One is by a cascade process, making use of the Single and Double Ion Ground States, and possibly the metastable states as intermediate levels in the excitation. The other is direct excitation without intermediate steps, and this is the more probable process during the first part of the spark discharge.

The multitude of ions formed by excitation perform cascades of transitions, each particle giving out a set of spark lines, and somewhat later, a set of arc lines. The overall effect is thus a displacement in time between the peak intensity of a spark line and that of an arc line. This displacement is clearly demonstrated in the intensity patterns which follow.

It may be here remarked that the instantaneous intensity observed in the patterns will accurately represent the instantaneous population of the origin level, because the lifetime in any level (other than the Ground States) is small compared to the resolution time of the pickup apparatus.

3. A typical intensity pattern for a spark line is diagrammed in Fig 20. Intensity is plotted vertically and time is measured horizontally from the beginning of the flow of spark current. The 5 microsecond time marks are here drawn approximately as they appear in the oscillograms to follow. G is the period of growth during which

Fig 20

TYPICAL SPARK LINE INTENSITY PATTERN

B. Initial Light Burst

G. Growth Period

P. Peak of Intensity Curve

t_p Peak Time

D. Decay Period

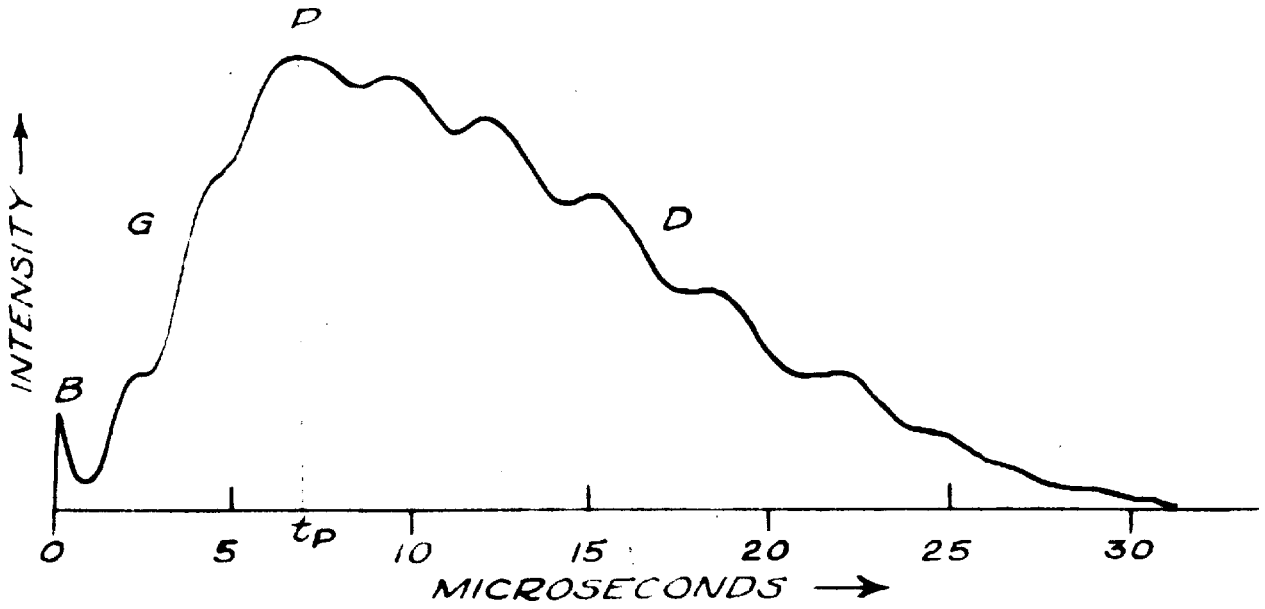
D
G
D
B
INTENSITY
0
5
t_p
10
15
20
25
30
MICROSECONDS

the spark gap is being filled with electrode vapor and the population of excited ions is growing in the origin. The peak intensity P occurs at the peak time t_p when the origin population has reached a maximum. D is the decay period which frequently exhibits a wavy character due to the alternating nature of the spark current. The initial burst B sometimes present in the intensity patterns is of very short duration, and is discussed in section D of this chapter. It does not belong to the spectral lines but must be considered as background light.

B. Arc and Spark Lines

1. Fig 21 shows oscillograms of intensity patterns at the left, and corresponding spark currents at the right for A an iron arc line, B an iron spark line, and C a nitrogen spark line. D shows the nitrogen line on a faster horizontal sweep. The time scale is given by the 5 microsecond marking pulses. Current waves are almost identical for A, B and C, but striking differences are seen in the intensity waves.

2. The arc line shows slow growth, rounded peak and rather late decay. The light is emitted from a cloud of excited vapor which is ejected from the electrodes. This light may persist for long periods, sometimes up to 10^{-3} seconds after the end of the discharge[13], spark lines being

Fig 21

OSCILLOGRAMS OF TYPICAL INTENSITY PATTERNS (left)
AND CURRENT WAVES (right)

In all cases I_{pk} = 320 amperes and F = 0.3 Megacycles for the current waves. Intensity patterns are for the following spectral lines:

A. 3059.09 Fe I a^5D_3 - $y^5D^o_4$

B. 3227.75 Fe II $a^4P_{2\frac{1}{2}}$ - $z^4D^o_{3\frac{1}{2}}$

C. 3329.5 N II

D. Same as C at 15 microsecond sweep.

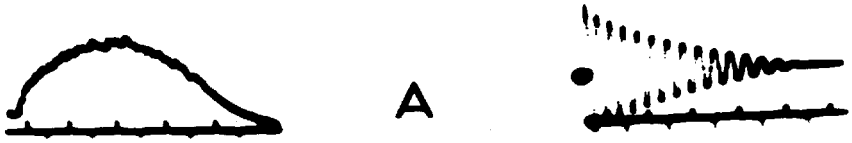
A

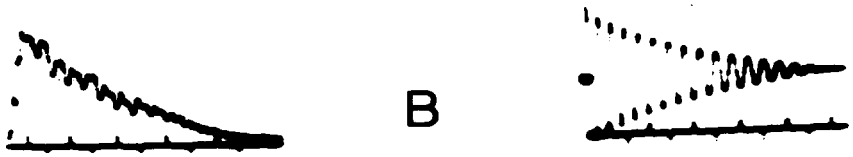
B

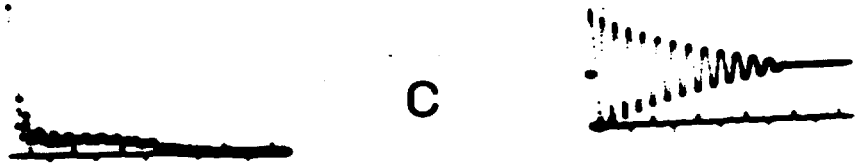
C

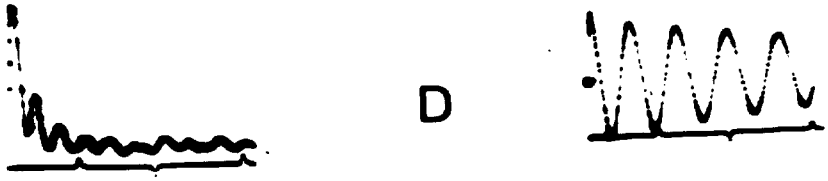
D

given off for a very short time, and arc lines for a much longer period. This indicates a considerable "inertia" in origin popultaion for arc lines. In particular it indicates that there is little population of the origin level directly by current excitation. The more probable mechanism of populating this low origin level, having an excitation potential here of only 4.086 volts, is by ions previously excited to higher levels which then tumble through a cascade of transitions into the origin level. The fact that only very small oscillations in intensity are present which correspond with pulses of spark current is further evidence in this view.

3. The iron spark line intensity pattern, B in Fig 21 shows fairly rapid growth, sharper peak, shorter peak time and earlier decay than the arc line pattern. Light from spark lines falls almost to zero at the conclusion of the discharge period. It indicates less population inertia in the higher origin levels associated with spark lines. The intensity pattern also exhibits some oscillations at twice the spark discharge frequency, which again is a low inertia property.

In considering the mechanism of populating the spark line origin, it may be assumed that this is partly by direct excitation and partly by ions cascading down from higher levels. The cascading time in this case is obviously smaller than

for an arc line since the spark line origin level is still fairly high. The excitation potential of the 3227.75 Fe II line is 13.317 volts.

The rate of growth in intensity of metal spark lines is limited by the rate of evaporation of electrode material into the gap, and hence one would not anticipate much decrease in peak time even for very high level lines. This was confirmed by observing the Cr IV line at 3172.08 Å having an excitation potential of more than 30 volts. This line showed an intensity pattern which was quite similar to those of the Fe II lines studied.

4. In contrast to the above, the rate of growth of the nitrogen spark line, C and D in Fig 21, does not depend upon the build up of a vapor density since the nitrogen is already there at the beginning of the discharge. This line shows rapid growth, sharp peak, and rather rapid decay to a low value after only a few current pulses. The rapid decay is immediately associated in time with the growth of the iron spark line intensity, and has the simple explanation that air density in the gap is rapidly reduced as electrode vapor is generated. This results in the presence of less nitrogen atoms available for excitation.

The remarkably low inertia of origin population for the nitrogen line is demonstrated in D of Fig 21. The intensity returns to a low value between pulses of spark current. It thus has a character, similar to that observed

by Dieke[16] for iron spark lines at comparatively low discharge frequencies.

While viewing the intensity pattern for the nitrogen spark line, a stream of argon gas suddenly directed between the electrodes of the sample gap caused the intensity pattern to drop at once to zero. This confirmed that the line had been properly identified as nitrogen and was not due to any electrode material.

5. The character of arc and spark lines thus gives us some significant information as to the mechanism of excitation. With the first few oscillations of current (5 to 10 microseconds), the electrode vapor density builds up to a maximum and is almost immediately excited by electron collision. Some cascade excitation may occur, but in general the atoms are excited to fairly high levels directly from the ground state.

More excitation of the higher energy levels may be expected to occur in the cathode region where electron temperature is high. By dissecting the light of the high level nitrogen spark line, it was possible to show that light from the region of one of the electrodes disappeared when this electrode became the anode, and reappeared when it became the cathode a half cycle later. The resulting intensity pattern was then similar to D in Fig 21 except that all the odd numbered pulses of light were missing. Light from the region of the other electrode showed the

same patterm with the situation reversed.

C. Optimum Bandwidth

As mentioned in Chapter III there is an optimum bandwidth for the intensity patterns which is a compromise between reduction of the noise and loss of detail in the signal. Since rather fine detail and good reproducibility was exhibited by the N II line, this is used to illustrate the choice of bandwidth. In Fig 22, 5 pairs of oscillograms show light intensity on the left and spark current on the right. Source conditions were the same for each oscillogram, and the bandwidth of the phototube system was increased going from A to E. Multiple exposures of about 30 shots each were made in each case in an attempt to cancel out the source fluctuation. It appears from this series that the detail of the intensity pattern is not much impared as the bandwidth is reduced to one megacycle. It may also be noted that the current wave showed remarkable reproducibility over the ½ second period of the exposure.

D. Background Light

It has been observed with photographic methods that troublesome background light is obtained on spectrograms when very large spark currents are used. The character of

Fig 22.

INTENSITY PATTERNS AT DIFFERENT BANDWIDTHS

Oscillograms of a N II line (left) and Spark Current (right). In each case the exposure was ½ second giving about 30 superimposed patterns. Source conditions were the same as in Fig 21. Bandwidths for the intensity patterns are as follows:

A. 0.1 Megacycle

B. 0.3 Megacycle

C. 1.0 Megacycle

D. 3 Megacycles

E. 10 Megacycles

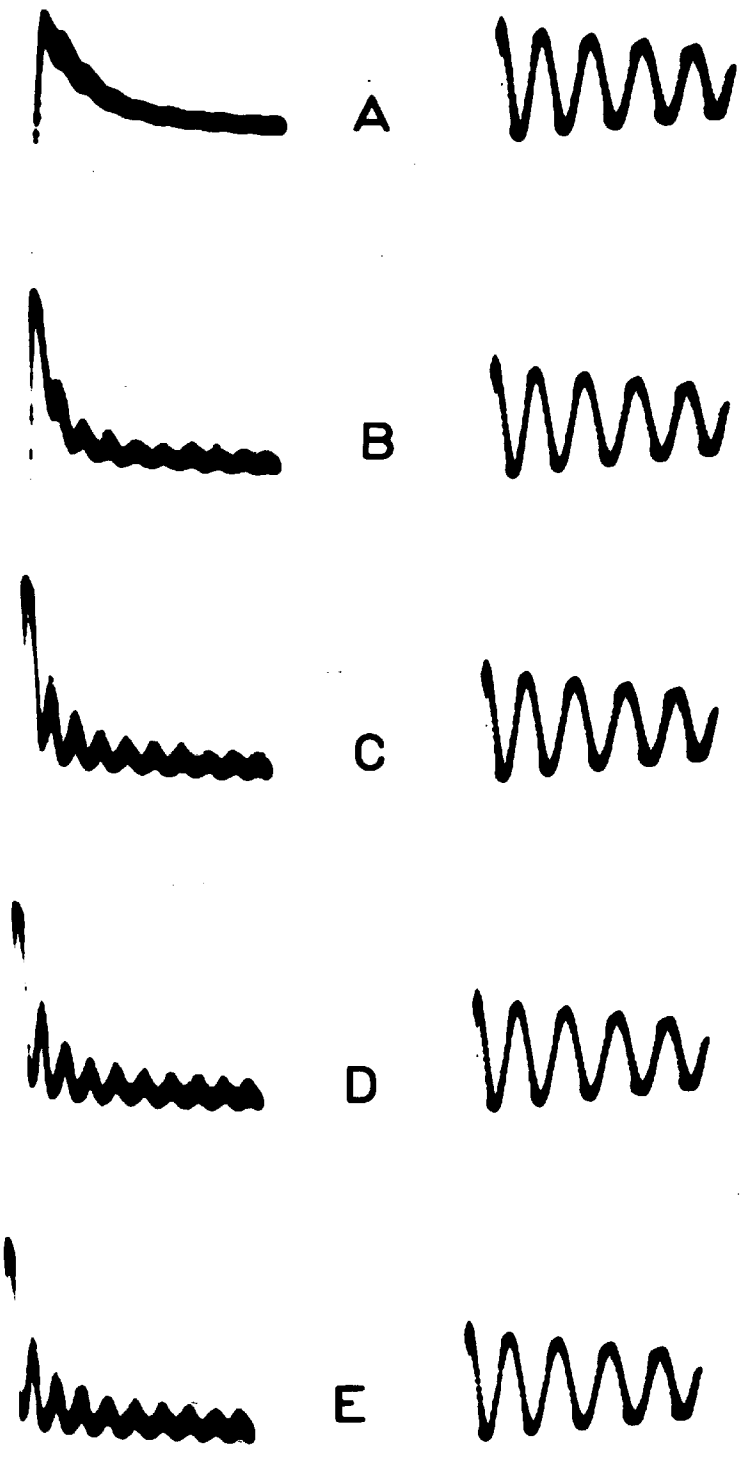
A
B
C
D
E

this background has not been well understood.

In making observations on spectral lines at high peak currents it was noticed that a sharp initial burst of light, B in Fig 20, was often present at the beginning of the discharge. The burst does not appear to be associated with any line since it persists when the slit is moved off the line. The burst shows quite singular character, reaching a maximum intensity almost immediately, and in the absence of a spectral line, returns to a small value in one microsecond. Its intensity is a sensitive function of peak spark current, a high peak intensity being obtained at I_{pk} = 700 amperes, and less than 10% of this value at I_{pk} = 300 amperes.

The peak intensity appeared to be unaffected by using different electrode materials in the sample gap. Pure copper, pure carbon, brass, zinc and iron were used with no change. This was also unaffected by a stream of argon or methane gas directed across the sample gap.

The light was dissected to determine if there existed a preferential region in the gap where the burst was strongest. A quartz lens was used to form an image of the gap on the entrance slit of the spectrograph. A 5 step Hartmann diaphragm was then used to examine different regions of the gap. No preferential region was found.

The burst was observed to be strongest in the 3300 to 5500 Å region of the spectrum, and was reduced in intensity

outside of this region. The fall off above 5500 Å coincides approximately with the response of the phototube in this region. The fall off below 3300 Å corresponds roughly with the energy distribution which is found for an incandescent body.

It is therefore believed that the burst is due to incandescence in the gas between the electrodes, producing a continuum. A continuum is not produced in air at atmospheric pressure, and it is therefore assumed that during the burst, a high pressure is built up in the gas filament through which the first pulse of current flows. The resulting small explosion also accounts for the rapid decay in the light, and also for the greatly increased sound generated at high peak currents.

E. Fluctuation in Intensity Pattern

1. General. In studying the fluctuation in light intensity patterns with phototubes, two facts must be mentioned. First, the phototube noise, if sufficiently large, may mask the effect being studied. Second, the effect of fatigue in the phototube may indicate a false gradual decay in light intensity.

Neither of these facts appear to be serious limitations to the fluctuation studies. The bandwidth may be reduced to improve the signal to noise ratio if necessary, and fatigue over the short intervals used in the fluctuation studies

appears to be negligibly small.

2. Methods of Recording Fluctuation. To record the nature and extent of fluctuation in the intensity pattern, two methods may be employed. If time exposures of the pattern are made using continuous gating to isolate one spark, the envelope thus formed by multiple exposure will then define the extent of the fluctuation. Alternatively a moving film record of the patterns may be made, and the images examined successively.

In the time exposure method, a half second exposure giving approximately 30 shots appeared to produce a satisfactory result. If this is a representative sampling, one should expect to obtain the same envelope for different half second exposures. Fig 23 shows three such time exposures of a half-second each on an iron spark line at one megacycle bandwidth. It can be seen from the similarity of these intensity envelopes that a half-second sampling time appears to be adequate.

Moving film records of intensity patterns were made on iron spark lines, and for some conditions these indicated a considerable fluctuation in peak time and general character from one spark to the next. This is not indicated in the time exposures which show only the extent of the fluctuation.

3. Fluctuation and Inductance -- Spark Line. The intensity pattern for the 3227.75 Fe II line was studied

Fig 23.

REPRODUCIBILITY OF FLUCTUATION PATTERNS

Each spectrogram of light intensity is a $\frac{1}{2}$ second exposure on an iron spark line giving approximately 30 shots. Source conditions were:

E_o = 160 volts

R_o = 10 ohms

C = .0107 microfarads

L = 4 microhenries (circuit inductance)

F = 0.83 megacycles

R_1 = 0

E_{pk} = 13 kilovolts

I_{pk} = 710 amperes

Sparks per half cycle = 2

Horizontal Sweep = 15 microseconds

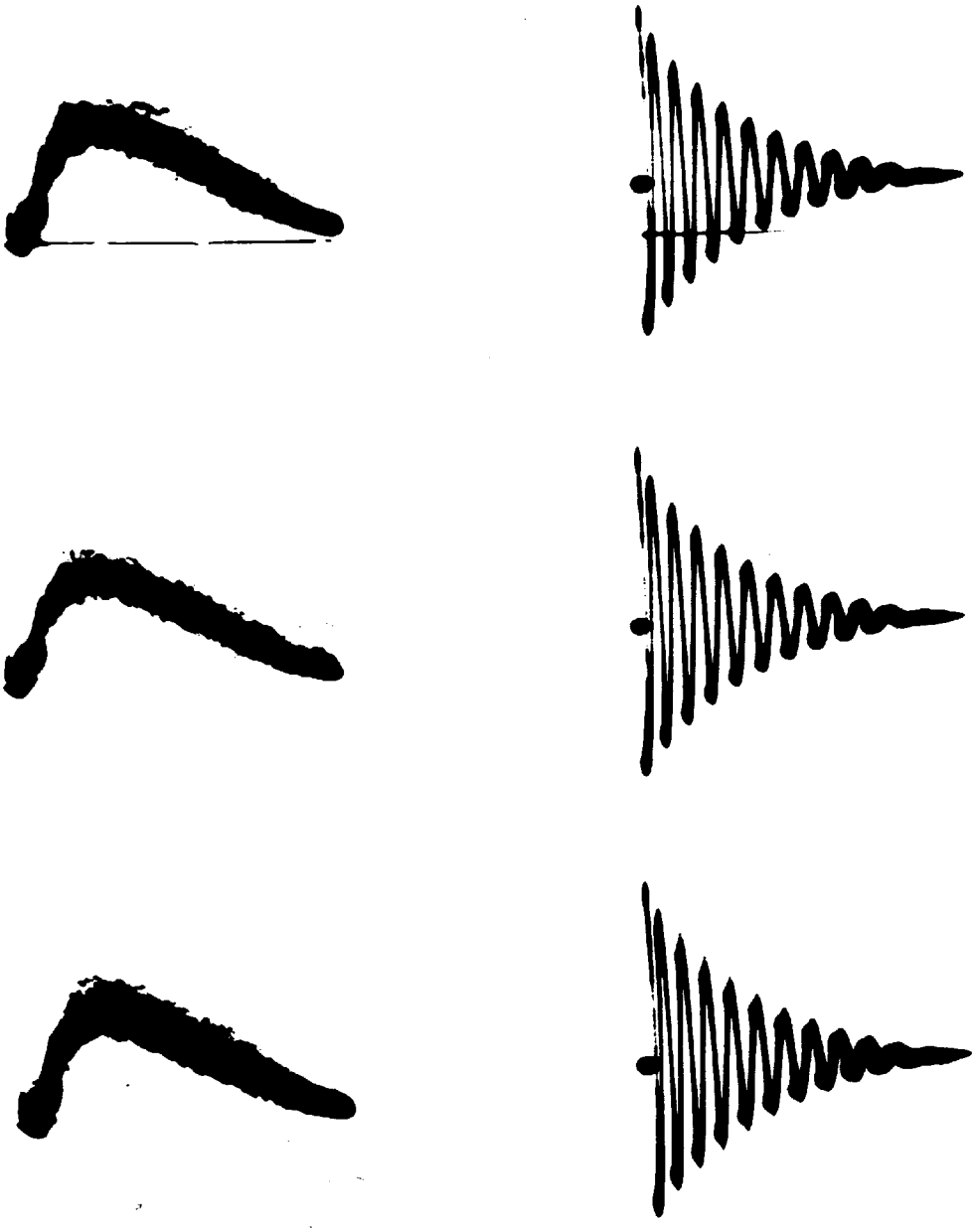

at different values of circuit inductance. It was desired to find out what relation, if any, existed between the inductance and the reproducibility of the intensity pattern with a steady spark current. Half-second exposures were taken at four values of circuit inductance, and the oscillograms are reproduced in Fig 24. The unchanged circuit conditions were as follows:

E_o = 160 volts

R_o = 10 ohms

Sparks per half cycle = 2

R_1 = 0

R_2 = .226 ohms

C = .0107 microfarads

E_{pk} = 13 kilovolts

Sample Gap = 3 mm Fe pins

Control Gap = 4.5 mm W pins

The inductance used in each oscillogram, and the resulting observed circuit conditions are given in the following table.

Table for Fig 24

Oscillogram	L_1 turns	I_{pk} amps.	F Mc/s	I_{RF} amps.
A	0	710	.83	13.0
B	5	460	.49	12.5
C	10	320	.30	11.0
D	20	220	.20	9.5

Fig 24

FLUCTUATION OF IRON SPARK LINE
WITH CHANGING INDUCTANCE

A. No added inductance

B. 5 turns added inductance

C. 10 turns added inductance

D. 20 turns added inductance

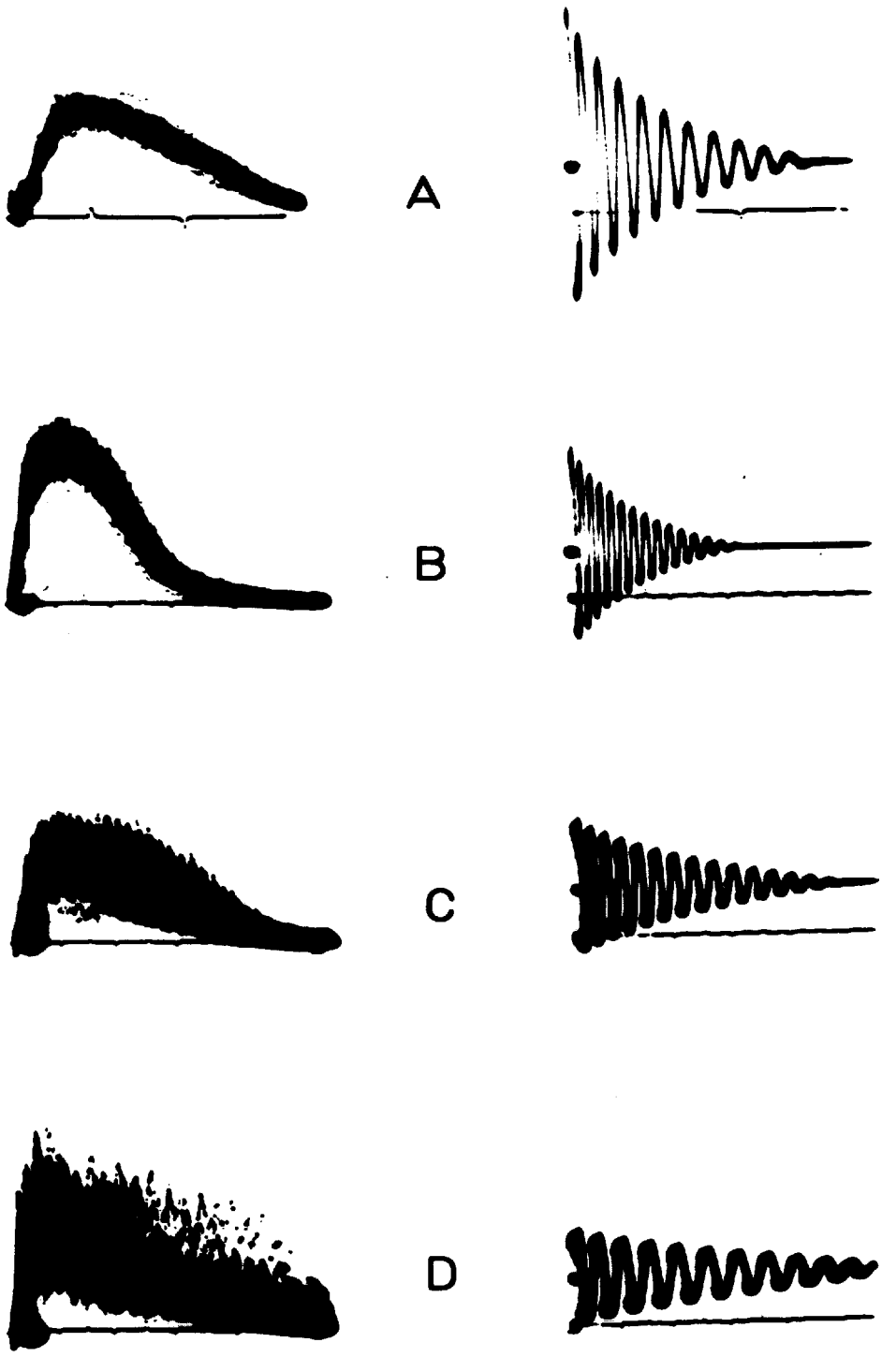
A
B
C
D

The oscillograms indicate that the fluctuation in intensity was least when the inductance was a minimum. Different attenuations were used in the various intensity patterns. Attenuation factors were 4:1 for A, 2:1 for B and C, and 1:1 for D. Taking account of this it was noted that the mean peak intensity varied roughly as $(I_{pk})^n$ with n having a value of 1.3 for the conditions used here.

Moving film records of intensity patterns on iron spark lines were made under different source conditions resulting in the following information.

(a) Fluctuation in the general shape and height of the patterns appears to be a true random process with no apparent dependence upon previous events.

(b) Fluctuation in peak time is quite small with minimum inductance, but increases rapidly as small amounts of inductance are added to the discharge circuit.

(c) Fluctuation in peak intensity even under the best conditions (minimum inductance) is very large during the "pre-burn" time, (the first 10 or 20 seconds after freshly grinding the electrodes).

An explanation of these three points will now be given on the basis of the observation of Kaiser and Wallraff[13] that the light is emitted by a vapor cloud ejected from the electrodes in a direction which frequently deviates from the discharge path, or core of the current.

(a) The cloud is ejected in a manner and direction controlled largely by the microscopic surface conditions of the cathode at and near the cathode spot. Since in general there is random motion of these spots over the surfaces of the electrodes, different microscopic conditions exist for each new spark, and intensity fluctuation of a purely random nature results.

(b) Since the vapor cloud may be ejected in almost any direction, different excitation timing will arise if it is ejected into the hot core of the discharge than if it is not. This gives rise to the fluctuation in peak time.

With minimum circuit inductance, resulting in a short discharge period, the spark current pulses have died down to perhaps 50% of the peak value by the time maximum vapor density is established. By then the bulk of excitation is completed, regardless of the direction of the vapor cloud. It is true that excitation will continue after this time, but to a much less intense degree. This is therefore a situation resulting in only small peak time fluctuation, the peak intensity always occuring a very short time after the maximum vapor density is obtained.

(c) A freshly ground electrode surface is covered with very small sharp ridges and valleys. After running in the spark for 20 seconds, the surface is in general much smoother.

Because of the greater irregularity of surface of the electrodes in the pre-burn period, and because of the considerations in (a) above, a greater intensity fluctuation results.

Fluctuation is also caused by a different geometry in the optical paths when the vapor cloud is formed in different shapes and positions. The result is a varying amount of light entering the spectrograph for a series of sparks having the same total luminous flux. The fluctuation from other causes is at least an order of magnitude larger than that due to geometry. This need only be considered when methods are found to decrease fluctuation from other causes by at least an order of magnitude.

4. Fluctuation and Inductance -- Arc Line. A similar fluctuation study for the 3059.09 Fe I line is reproduced in Fig 25. Source conditions for the four oscillograms are the same as for Fig 24, but considerably more fluctuation was observed in all cases. Attenuation was the same for all four patterns indicating that a mean peak intensity of an arc line is relatively insensitive to peak current increases above 320 amperes. However fluctuation was least with minimum inductance as before.

The initial burst discussed in Section D may be noted in A of Fig 25 at the high peak current of 710 amperes.

Fig 25.

FLUCTUATION OF IRON ARC LINE
WITH CHANGING INDUCTANCE

A. No added inductance

B. 5 turns added inductance

C. 10 turns added inductance

D. 20 turns added inductance

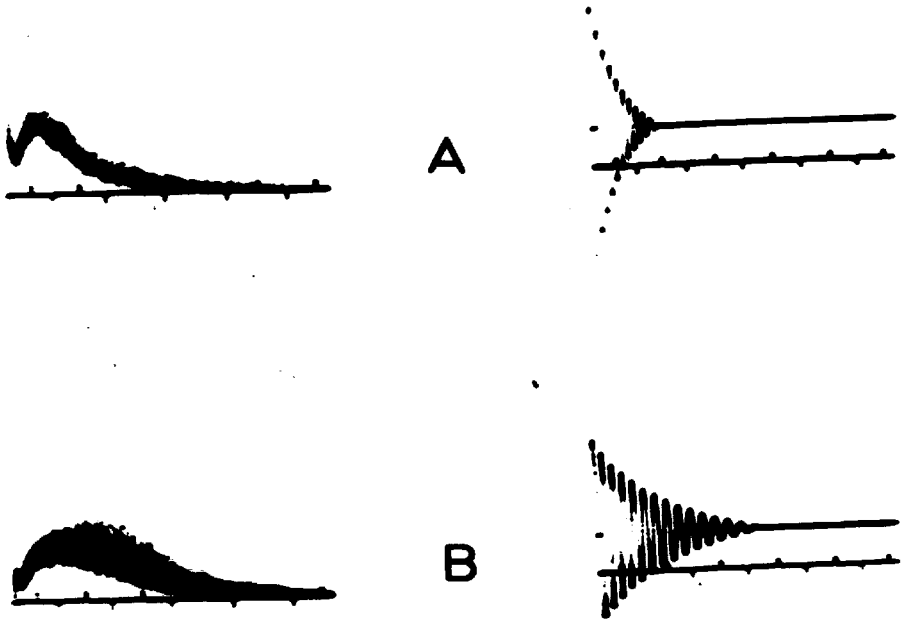
A
B
C
D

5. Fluctuation and Capacity -- Spark line. Fig 26 shows fluctuation of the 3227.75 Fe II line with changing capacity. The same attenuation was used in all intensity patterns. In E a non inductive resistor of one ohm was added to the discharge circuit giving R = 1.3 ohms. The fixed source conditions were as follows:

R_o = 10 ohms

R_2 = .226 ohms

L_1 = 0

L = 4 microhenries (circuit inductance)

E_{pk} = 13 kilovolts

Sample Gap = 3 mm Fe pins

Control Gap = 4.5 mm W pins

Due to different charging time constants as C was varied, it was necessary to adjust E_o to produce a steady number of sparks per half cycle. The observed circuit conditions with different values of C are given in the following table.

Table for Fig 26

Oscillogram	R (total) ohms	C ufd.	Breaks per ½ cycle	I_{pk} amps.	F Mc/s	I_{RF} amps.
A	.3	.00255	4	270	1.6	6.8
B	.3	.00462	3	370	1.3	8.5
C	.3	.00612	3	425	.97	9.5
D	.3	.0107	2	710	.82	13.5
E	1.3	.0107	2	710	.80	13.0

Fig 26.

FLUCTUATION IN IRON SPARK LINE
WITH CHANGING CAPACITY AND
RESISTANCE

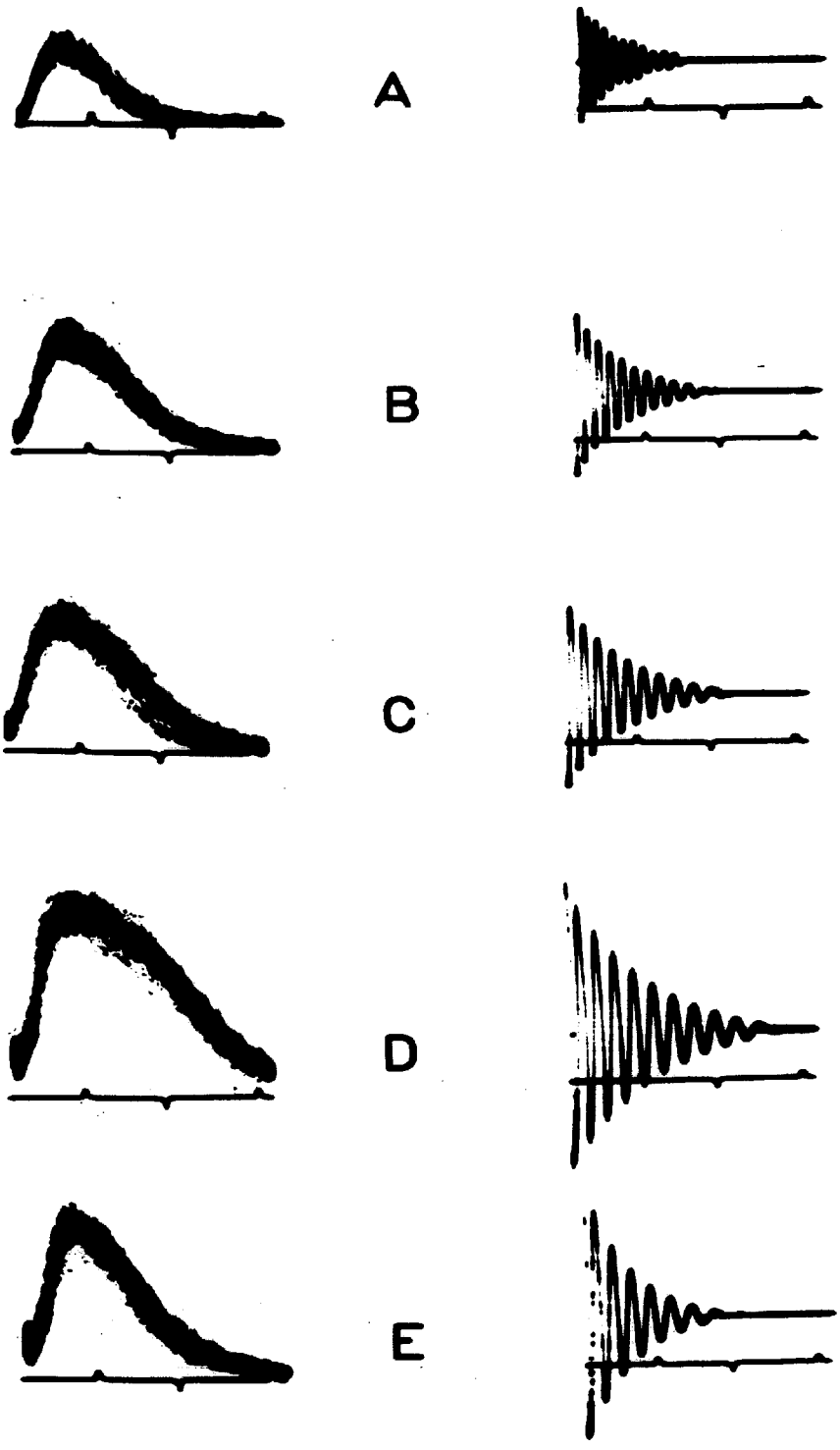
A
B
C
D
E

An examination of the fluctuation patterns indicates that although fluctuation appears smaller with lower capacity, the overall intensity is correspondingly reduced. Thus the relative fluctuation appears to be about the same for A, B, C and D. The effect of adding resistance in the discharge circuit is illustrated by comparing oscillograms D and E. Decay in the light is earlier in E, but the relative fluctuation appears to be about the same as in D. Other data indicated that a slight decrease in fluctuation is obtained with added resistance, but the evidence here is inconclusive. High wattage non inductive resistors larger than one ohm were not available to study a wider range in R.

VI. CONCLUSION

1. The study of the intensity structure of spectral light from a spark source gives considerable information about the mechanism of excitation, and also shows the way to reduce the fluctuation in light output. It is indicated that the most probable mechanism for large peak currents such as are commonly employed in quantitative analysis, is fairly high level direct excitation of the material present in the sample gap. A subsequent cascade of transitions ensues, so that population of the lower levels is largely by a downward cascade. This results in a delay in light emitted in a transition from a lower level, e. g. as in an iron arc line, and a population inertia effect which appears to increase with the lower levels.

The lifetime of an atom or ion in any intermediate energy level is so short that instantaneous light intensity of a spectral line gives a fairly accurate measure of its instantaneous origin population. In addition, any inertia effect observed in an origin level must be therefore attributed to the mechanism of populating this level. In general this mechanism is a downward cascade of particles from upper levels, and in particular, from the next highest Ground State where cascades are initiated, and where comparatively longer lifetimes exist.

Let us attempt to see how these inertia effects arise. Let t be the average lifetime of particles in the Single Ion Ground State. If a sudden increase is produced in the population of this level at time zero, there will be no appreciable increase in rate of cascade initiation until about the time t. If we consider the effect of this upon one of the lower levels, it will be seen that its population will respond only sluggishly since an appreciable change in the population will occur only after the time t. The result is an apparent inertia in the level just considered.

t is comparatively large for the Single Ion Ground State, and this results in a high inertia for arc lines. By comparison, the corresponding t for the Double Ion Ground State is small, resulting in a lower inertia for spark lines.

By a further study of the intensity structure of spectral light, it would be possible to calculate these lifetimes accurately. However the problem would be complicated in the case of the spark source because of the fluctuation in peak time. The most that could be done in this case would be to use mean values of peak time as was done in the fluctuation studies, or confine the work to those conditions where only a small fluctuation in peak time is observed.

2. The course of events in the discharge period is as follows. When the spark first strikes, the gas present between the electrodes is heated very rapidly to incandescence, if a high peak current is used. This produces a burst of light, and a high pressure is momentarily built up resulting in a small explosion. The burst of light rapidly disappears as pressure equilibrium is restored. This occurs in less than one microsecond after the striking of the spark. The burst is very sensitive to peak current and was not detected without employing fairly high currents.

The first few oscillations of spark current excite the air in the gap resulting in the emission of air lines. Of these, the nitrogen spark lines are quite strong and easily studied. Their intensity reaches a peak which is almost coincident with the peak current, and for each pulse of current a pulse of light is produced, the intensity falling to a low value between current pulses.

The first few current pulses produce very hot cathode spots on the electrodes, which eject a vapor cloud. During this period, the air lines are rapidly reduced in intensity to a low value as the gap fills with electrode vapor, and the intensity of spark lines of the vapor build up to a maximum in 4 to 10 microseconds. The intensity of the arc lines of electrode material grows more slowly, a mean peak intensity being reached in 10 to 40 microseconds. For

the same electrical conditions, the mean peak time for arc lines is always larger than for spark lines.

The nitrogen spark lines disappear before the end of the discharge period, while metal spark lines remain a few microseconds after the end of the period. Arc lines decay slower and last much longer, sometimes persisting for 25 microseconds after the discharge ends.

3. The peak intensity of iron spark lines increases rapidly as the peak current is increased, but that of iron arc lines increases only slightly above 300 amperes peak current.

4. Fluctuation in spectral light intensity patterns is caused chiefly by differences in the manner and direction in which the vapor cloud is ejected from the electrodes. When the vapor cloud is directed into the hot core of the discharge, there results different timing and extent of excitation of the vapor than otherwise.

Intensity fluctuation may also be produced in the spectrograph by differences in the optical paths from one spark to the next, but in general this is of lower magnitude than fluctuation otherwise produced.

Fluctuation differs with different types of spectral lines under the same source conditions being large for arc lines, smaller for spark lines, and least of all for high level nitrogen spark lines. It therefore appears that those atomic processes which occur most rapidly exhibit the least

fluctuation.

5. Fluctuation in iron arc and spark lines is reduced when the discharge time is reduced by decreasing the circuit inductance. It therefore appears that an electrical process which occurs in the shortest time also produces the least fluctuation. It is therefore concluded that to reduce fluctuation in these lines, the excitation process should be kept as short as possible. To do this most efficiently, the spark circuit inductance should be reduced to a minimum. This produces a high peak current, a high discharge frequency and a short discharge period.

BIBLIOGRAPHY

1. O. S. Duffendack and W. E. Morris
J. Opt. Soc. Am. 32, 8, (1942)

2. J. L. Saunderson, V, J. Caldecourt and E. W. Peterson
J. Opt. Soc. Am. 35, 681, (1945)

3. M. F. Hasler, R. W. Lindhurst and J. W. Kemp
J. Opt. Soc. Am. 38, 789, (1948)

4. Ford R. Bryan and George A. Nahstoll
J. Opt. Soc. Am. 38, 510, (1948)

5. H. B. Vincent and R. A. Sawyer
J. Opt. Soc. Am. 32, 686, (1942)

6. Hoskins Manufacturing Co., Detroit, Mich.
Catalog L, Page 33

7. I. E. Lampert and R. Feldt
Proc. I. R. E. 34, 432 (1946)

8. F. E. Terman, Radio Engineers' Handbook pp418-422
1st Ed., McGraw-Hill 1943

9. W. R. Hill, Jr.,
Proc. I. R. E. 33, 38, (1945)

10. K. G. Kessler and R. A. Wolfe
J. Opt. Soc. Am. 37, 133, (1947)

11. G. H. Dieke and H. M. Crosswhite
J. Opt. Soc. Am. 35, 471, (1945)

12. J. H. Enns and R. A. Wolfe
A. S. T. M., Tech. Pub. No 76 (1948)

13. H. Kaiser and A. Wallraff

Ann. d. Physik, 34, 297, (1939)

14. H. Barkhausen

Ph. Zeitschrift, 8, 624, (1907)

15. D. R. Roschanski

Ann. d. Physik, 36, 281, (1911)

16. G. H. Dieke, H. V. Loh and H. M. Crosswhite

J. Opt. Soc. Am. 36, 185 (1946)

APPENDIX

VOLTAGE REGULATOR OPERATION AND ADJUSTMENT

Fig 27 shows the circuit of the compensated voltage regulators used in the power supplies where stable voltages were required. When properly adjusted, the output voltage E_o contains less than three millivolts of ripple although a volt or so may be present in the input voltage E_1. The long period variation of E_o is less than 0.1 volt.

An expression for the regulation factor $\partial E_o/\partial E_1$, in terms of the circuit and tube parameters is given by Hill[9]. This expression may be made zero by a proper choice of circuit constants. In practice the regulation factor may be made to approach zero over limited ranges of input voltages and load currents, and may be made negative if desired.

The circuit may be regarded as a DC amplifier T2 with large negative feedback and cathode follower output T1. Since the only amplifier input is the negative feedback voltage, the resulting output impedance is low and the output voltage is substantially constant. T3 is a cold cathode, voltage reference tube whose operating current is adjusted to the proper value by a suitable choice of R5. The cathode of T2 is held at a steady reference potential E_3, and a fraction E_2 of the output voltage is compared to E_3 by the amplifier.

With R4 = 0, there is a small regulation factor, usually

Fig 27

COMPENSATED VOLTAGE REGULATOR CIRCUIT

Typical values are as follows:

E_1 = 350 volts

E_o = 250 volts

R_L = .1 Meg ½ watt

R1 = .1 Meg Pot

R2 = 47 K ½ watt

R3 = .2 Meg ½ watt

R4 = 5 K Pot

R5 = 10 K 10 watt

T1 = 2A3

T2 = 6SJ7

T3 = OC3/VR105

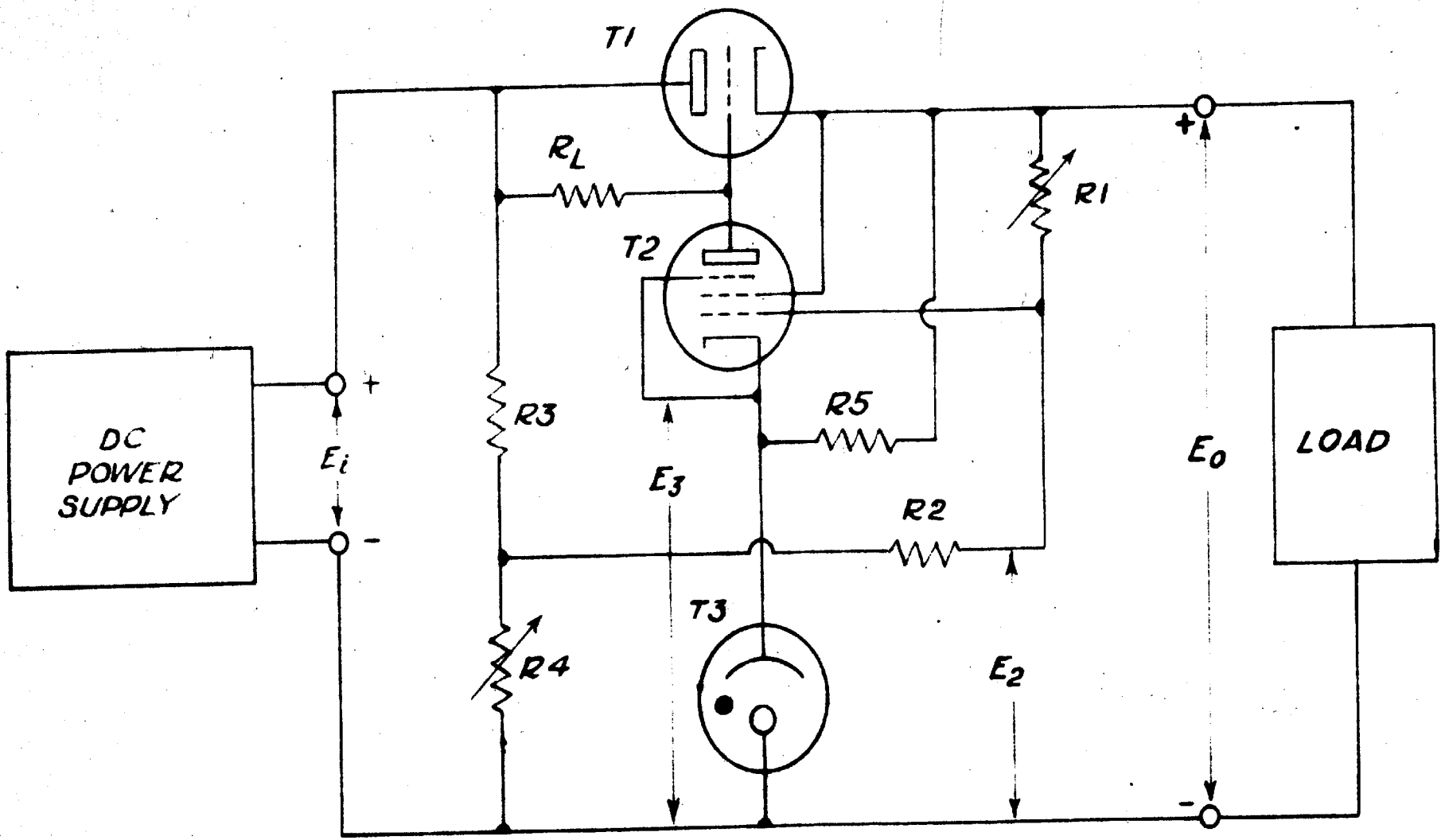
T1
R_L
T2
R1
+
R3
R5
DC
POWER
SUPPLY
+
E_i
-
E_3
E_o
LOAD
R2
T3
R4
E_2
-

about .01, but if the proper fraction of input fluctuation is applied to the amplifier grid, output fluctuation disappears. This fraction is obtained by the divider R3 and R4. When R4 is properly adjusted, a regulation factor of zero may be obtained, in theory at least, giving complete compensation for input voltage changes.

In practice the adjustments to the circuit are made as follows. R1 is adjusted to produce the required output voltage. The compensation is then adjusted by varying R4 until no ripple appears in the output. It is usually necessary to introduce a few volts of ripple in the input to obtain a satisfactory compensation adjustment.

Compensation for changes in load current may also be made by a simple addition to the circuit, and this is also discussed by Hill[9]. This addition was not required here since all loads were substantially constant.